RA:dOst
Regionale Anpassungsstrategien für die deutsche Ostseeküste

# REPORT

# COMPARING THE "BATHTUB METHOD" WITH MIKE 21 HD FLOW MODEL FOR MODELLING STORM SURGE INUNDATION

-Case Study Kiel Fjord-

Tim Neumann, Kai Ahrendt

RADOST-Berichtsreihe
Bericht Nr. 22
ISSN: 2192-3140

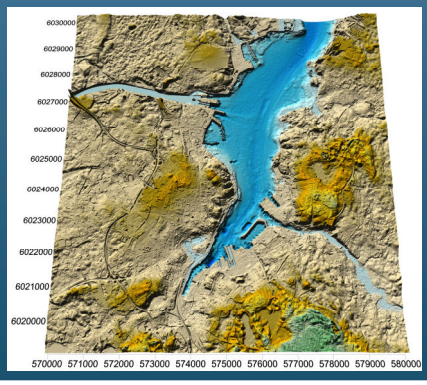

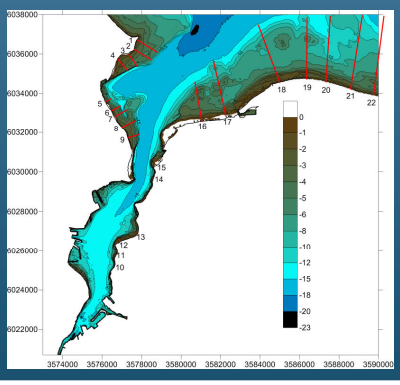

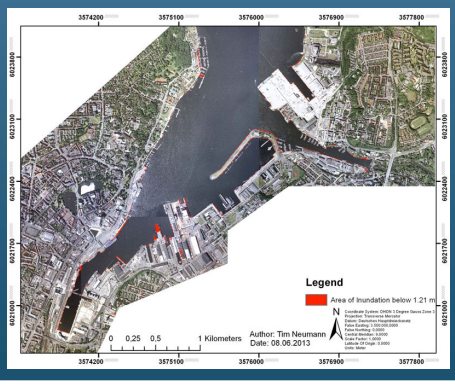


GEFÖRDERT VOM
Bundesministerium für Bildung und Forschung
KLIMZUG
Klimawandel in Regionen

## Kooperationspartner

Büro für Umwelt und Küste, Kiel
**BfUK**

Leibniz-Institut für Gewässerökologie und Binnenfischerei, Berlin
**IGB**

Geographisches Institut der Christian Albrechts-Universität zu Kiel
**CAU**

Leibniz-Institut für Ostseeforschung Warnemünde
**IOW**

Coastal Research & Management, Kiel
**CRM**

Institut für ökologische Wirtschaftsforschung, Berlin
**IÖW**

Ecologic Institut, Berlin (Koordination)
**Ecologic**

Landesbetrieb Küstenschutz, Nationalpark und Meeresschutz Schleswig-Holstein, Husum
**LKN**

EUCC – Die Küsten Union Deutschland, Warnemünde
**EUCC-D**

Landesamt für Landwirtschaft, Umwelt und ländliche Räume Schleswig-Holstein
**LLUR**

GICON – Großmann Ingenieur Consult GmbH – Niederlassung Rostock
**GICON**

Staatliches Amt für Landwirtschaft und Umwelt Mittleres Mecklenburg
**StALU MM**

H.S.W. Ingenieurbüro Gesellschaft für Energie und Umwelt mbH, Rostock
**HSW**

Johann Heinrich von Thünen-Institut, Bundesforschungsinstitut für Ländliche Räume, Wald und Fischerei, Braunschweig
**TI**

Helmholtz-Zentrum Geesthacht, Zentrum für Material- und Küstenforschung
**HZG**

Technische Universität Hamburg-Harburg, Institut für Wasserbau
**TUHH**

Institut für Angewandte Ökosystemforschung, Neu Broderstorf
**IfAÖ**

Universität Rostock, Fachgebiet Küstenwasserbau
**URCE**

# REPORT

# COMPARING THE "BATHTUB METHOD" WITH MIKE 21 HD FLOW MODEL FOR MODELLING STORM SURGE INUNDATION

-Case Study Kiel Fjord-

Bachelor Thesis, Geographisches Institut Universität Kiel

Tim Neumann
Geographisches Institut der Universität Kiel

Dr. Kai Ahrendt
Büro für Umwelt und Küste, Kiel

RADOST-Berichtsreihe
Bericht Nr. 22

ISSN: 2192-3140

Kiel, Dezember 2013

# Content

**Figures**



**Tables**

# Abstract

Meteorological measurements in the past showed that the climate is changing rapidly over the last decades with an increasing tendency. It is expected that this trend will further increase in the future. Therefor there is a growing interest in understanding corresponding effects. One of the most challenging effects are floods. Due to the willing to evolve a sounder understanding of processes take place during an inundation event, there is an immense development of methods to analyse. This work deal with a comparison between the common "bathtub method" and a state-of-the-art hydrodynamic model, called MIKE21 HD Flow Model, for modelling storm surges. The aim of this study is to work out the differences between both approaches and to find out how probable differences look like. There is the question if the "bathtub method" represents flooding adequate or, if the consideration of physics by hydrodynamic models makes a major difference and displays maybe the "real" risk of inundations. This work tries to underline the differences between those two approaches, where the strengths and weaknesses are and what influence those differences have for an inundation analysis. The investigation was made on a digital elevation model for the study area of Kiel, the capital city of the state Schleswig-Holstein in Germany. It is a midsize city of 242.041 inhabitants in the south-west of the Baltic Sea. The two approaches were made on data for a small storm surge on the basis of water-level-change and wind-regime data from 2010. The major aspect of investigation was the inundation extend under applying the different approaches. Water-level changes were implemented by developing different scenarios and additionally using time series from a surge for simulations. Further it was examined what influence surface resistance could have for the study area and how this influences the outcome of the two approaches as well as how inundation changes by taking physical behaviour of water-surface interaction into account. The results showed a difference between both approaches of average 11.25 % for a 2-D and 6.89 % for a 3-D surface analysis, where the "bathtub method" overestimates the hydrodynamic modelling (HDm). Further the outcome shows interesting behaviours when looking on different sea level rise scenarios what can be elucidated by changing resistances due to changing friction.

Concluding the outcomes of the work, they show a distinct difference between both approaches. Taking the HDm as "real", the "bathtub method" overestimates the area of inundation for a storm surge. But it has to be differentiated by different scenarios. Generally a shallower inundation seems to be more influenced by forces like friction than an event of higher water ¬levels. By arguing so, it should always be considered to use HDMs, at least to get a comparable result for an analysis. The outcome of this work can be seen as a hint for inundation analysis and how to grade analysis of those two approaches.

To make a more reasonable statement about the error of the approaches further effort should be done in future, to repeat this work on different case-studies.

# 1 Introduction

Since climate is changing rapidly the fear of natural hazards and damages increases. The most likely consequences to global warming are accelerated Sea Level Rise (SLR) due to thermal expansion and melting of ice as well as a change in meteorological regimes which can produce storm surges. The most threatening impacts are floods. “In 2011, floods were reported to be the third most common disaster, after earthquake and tsunami, with 5202 deaths, and affecting millions of people“ (Balica et al. 2013, p. 84). Also areas, which are apparently not at high risk, are threatened. Even Europe, which has a high adaptive capacity and a well-developed scientific base, will have to manage conditions previous not experienced and to cope with those problems on different ways (Nicholls & Klein 2005, p. 200). “One third of the European Union population is estimated to live within 50km of the coast“ (Nicholls & Klein 2005, p. 200; Nicholls & Klein 2005, p. 209). Comparing to other high threatening parts of the World, a high necessity to expand sea-level impact assessment is discernible as coastal regions become more vulnerable by changing boundary conditions (Poulter & Halpin 2005, p. 167). Due to this demand of information it should be the aim to apply the most reasonable approach to model and gain optimal results in terms of preciseness and accuracy to display inundation risk. To get this information environmental modelling is the common strategy to generate knowledge of future risks.

Models are generally a simplified representation of reality. Like a sculptor forms his physical model with a range of techniques and tools out of clay, a scientist does the same in mathematical manner with help of equations, based for example on a computer software. The problem on modelling is to have a sound understanding of what is going to be inspected. The highest task is, to observe the nature and to decide which aspects are important for further investigations. By this a model always shows just those components which are seen to be essential for the process. Thereby a model takes always the modellers signature. This can lead to a not completely objective perspective of the system (Wainwright & Mulligan 2004, p. 8). However, the biggest advantage on environmental modelling is a numerical precise hypothesis which than can be quantified and evaluated, what allows observations to be explained and future predictions to be made (Smith 2007, p. 4-7). In general, environmental modelling has the potential to:

1. quantify expected results
    - recent weather trends (do we expect sufficient rainfall over the summer)
2. compare the effects of two alternative theories
    - does an inundation reaches further inland when boundary conditions do have a stronger emphasis on wind conditions than on SLR
3. describe the effects of complex factors such as random variations in input
    - how do uncertainties in C02 trends affect predictions of future climate change
4. explain how the underlying processes contribute to the observed results
    - how changes in the quantity of one parameter can change the physical behaviour
5. extrapolate results to other situations
    - what would the inundation look like, if there would be an additional meter of wave height

6. predict future events

- if SLR will be 1,9 meter above MSL by 2100 the inundation will look like...

7. translate science into a form that can be easily used by non-experts

- weather forecast allows us all to make use of complex meteorological science

The use of environmental modelling is based on the context concerning climate change (Wainwright & Mulligan 2004, p. 1). They can develop and improve our understanding for environmental processes. Although most processes are not observable, their affects and effects are measurable and can be used for modelling. Therefor it is often difficult to distinguish between the environmental process and the outcome which is modelled incorrect. But it does provide at least a base for investigations (Wainwright & Mulligan 2004, p. 1).

Because there is such a huge margin of parameters in environmental modelling, parsimony is one of the highest principles. In a modelling context, parsimony means a high as possible explanation and simplicity while the complexity and amount of parameters should be as less as possible. “It is a particularly important principle in modelling since our ability to model complexity is much greater than our ability to provide the data to parameterise, calibrate and validate those same models. Scientific explanations must be both relevant and testable. Non-validated models are no better than untested hypotheses“ (Wainwright & Mulligan 2004, p.8).

To combat the problems of flooding, inundation modelling is done in different ways. The key task of all inundation assessments is to predict future water levels and inundation extent that result from particular trigging combinations such from meteorological and tidal conditions (Bates 2005, p. 794). Inundation modelling, which addresses the above mentioned problem of flood risks, has the aim to predict e.g. storm-induced coastal flooding on an accurate manner (Cheung et al. 2003, p. 1354). Methods combining geographical information systems (GIS), remotely sensed data and numerical models have been developed to deal with these difficulties and to understand flood risk (Wadey et al. 2013, p. 2). In the context of inundation modelling immense problems are uncertainties like the upcoming SLR. The Intergovernmental Panel on Climate Change (IPCC) estimates in its six “SpecialReport on EmissionScenarios“ marker scenarios (SRES) an upcoming SLR of 0.37m for the lowest estimation, named “B1“, to 0.58m, called “A1FI“ by 2100. This SLR will be based on thermal expansion and melting of ice (IPCC 2007, p. 323). However, to get an idea about this, the example of ice-sheet melting rates can demonstrate uncertainties. If these discharge rates are linear until 2100 there will be an additional SLR of 0.05m to 0.11m, which has to be taken into account for “A1FI“. Anyway, in sum this would lead up to 0.69m SLR (sum of the general SLR from A1FI of 0.58m plus ice melting of 0.11m), which is 86.5% more than the lowest assessment.

These numbers are of interest for long term investigations but don't have a huge effect for storm surge modelling nowadays, because "the annual SLR increment is about an order of magnitude smaller than the vertical error of most elevation datasets" (Poulter & Halpin 2005, p. 168). Furthermore the effect of changing meteorological-regimes due to climate change are classified and expected to be much more threatening in terms of temporal extreme water levels than SLR. Even this is strongly discussed and under worse assessable uncertainties (Graham 2008, pp. 197-198).

A more significant problem is the resolution of the digital elevation models (DEM), which are the basic data of environmental modelling whereas those data are the "playground" the modelling is based on. In general a DEM gets interpolated to a homogenous grid of a defined resolution e.g. 10x10m. Once this interpolation is processed the DEM may contains

significant topographic uncertainties in the surface (Marks & Bates 2000, p. 2110). This can results in a worse vertical accuracy. "Consequently, the model is of a much higher resolution than the basic topographic data set and, with rapid improvements in computational power, this situation is likely to get worse" (Marks & Bates 2000, p. 2110).

It is obvious that uncertainties do have an immense influence on what areas are modelled to be under inundation stress. Therefore Hulme et al. mentioned in the IPCC Assessment Report 4 (AR4), chapter 6 (Coastal systems and low-lying areas) that coastal impact scenarios should take additional 50% of the amount of mean SLR into account, plus local factors to the initial sea surface prediction to compensate uncertainties. Those factors could be local uplift or subsidence of the land (IPCC 2007, p. 324; Poulter & Halpin 2005, p. 170). The reason including these factors is to give coastal managers a higher potential sea level for their planning to gain extra safety in their undertakings of coastal management issues (Nicholls & Klein 2005, p. 211-214).

Two often applied approaches in inundation modelling are the "Bathtub Method" (BTM) and hydrodynamic modelling (HDm), which are going to be the approaches applied in this study. The main idea behind the BTM is, an area which lies under a certain height, gets flooded like a bathtub. An example is the flood warning system of the city Kiel (http://ims.kiel.de/extern/kielmaps/?view=katschu&) (Landeshauptstadt Kiel 2008). It gives inundated areas for a particular corresponding height. But this Kiel application is a web based GIS and it is strongly limited to the user. It is just a geographical presentation of different elevation levels. There are no possibilities for the user to produce own results. It just shows pre-produced results.

Rodriguez (2010) presents in his work "Mexican Gulf of Mexico Regional Introduction and Sea Level Rise Analysis of the Carmen Island, Campeche, Mexico Region" a way of how to work with a DEM and how to get information about inundations. A solution to determine inundation areas is to reclassify a DEM to the scenarios height, like Klein and Nicholls (1998) show in the example “Use of satellite data and GIS in a coastal impact assessment for Poland”. Rodriguez technique is much more detailed and gives more output to analyse, thus he also undertakes a 3-D analysis to generate numerical precise statements. He formulated his method to determine coastal effects for the region of Carmen Island in the Mexican Gulf of Mexico. His considerations were based on a, to global climate change associated, SLR estimation of 60cm by 2100. The coastal effects were investigated on the SRTM DEM of a resolution of 90x90m.

A result of his research was a two coloured map, showing areas which are equal or less then 60cm of height in one colour and the rest in another one. This new produced raster was superimposed on the original DEM and made transparent so the areas of inundation were apparent.

For final analysis of landmass loss, the above mentioned 3D-analysis was processed on the entire DEM to calculate the statistics. The results of the statistics were presented in tables (Rodriguez 2010, p. 1-18). The advantage of this approach is the dimensional analysis instead of just graphical interpretation like in the example of Kiel. Summarised a BTM inundation analysis is a four part framework:

1. First task: collect and generate data:
    - with special focus on DEM
2. Second step: pre-processing of the DEM, its parts and task are:
    - geo-referencing (to make sure analysis will be in the right spatial frame)

- if possible validating vertical values

3. Step three: prepare and analyse the DEM:
   - applying the Scenario (to get in detail selection for area of interest)
   - selecting area of interest
   - reclassification
4. The fourth step is analysing:
   - processing of maps, graphical analysis of inundation
   - spatial calculations of inundation

The approach of HDm is the second tool for developing coastal flood management policy which will be discussed here. The model, used in this study is the MIKE21 HD Flow Model by DHI (Danish Hydraulic Institute). In the case of assessing coastal hazards, 2-Dimensional horizontal solutions of the shallow water equations (SWE) are currently the state-of-the-art tools. In shallow seas, such as coastal bays and estuaries are, models which are based on those equations provide simulations of water levels in good realistic manner (Bates 2005, p. 794). The interactions between the medium and the earth surface are elementary components in the process of inundation. Due to the movement of water particles forces arise like currents which can emerge by the influence of wind. Wind also could lead to a changing wave regime. Different wave-wind-regimes obvious lead to different risk potentials. These factors are so called hydrodynamics and are considered in HDm.

However, like mentioned above, the resolution of the DEM is the most crucial point to gain acceptable results. Whereby the resolution should be more detailed the smaller the scale of the study area is. For example, in case of a damage appraisal on local scale, the computational grid should resolve 50m or less. For an observation on regional scale Bates et al. (2005) suggest a resolution of 200 - 50m. Anyhow it is difficult to distinguish between the process or the outcome which is simulated in a reasonable manner, to determine a sound understanding of the risk and risk providing parameters it has to be simulated a set of runs. Even though, the assumption of deterministic inundation modelling is highly questionable due to parameterisation and simplification in solving equations (Bates 2005, p. 794). To gain accuracy and significance there is the demand to evaluate and compare different sets of input-parameter which are maybe equal likely to determine computational demands. But by running different sets there is a growing workload on computing resources. Regarding this, the development of hydrodynamic models (HDM) gets improved in the direction to evolve systems which are capable to capture all essential physics to simulate substantial mechanisms of flooding, but at significant lower computational cost (Bates 2005, p. 794; Wainwright 2004, p. 8).

Anyhow like the BTM, a HDM is also just an assumption of reality. The SWE are an assumption which is derived from reality.

This work will compare this both approaches. The aim is to figure out, how the main differences, taken physics into account or not, are influencing the results of inundation simulations on the study area of Kiel. Three different scenarios were simulated, one is a small storm surge in the Baltic Sea, one additional with a weak SLR and one with additional a maximum SLR, to see different percentage variation of inundation comparing the HDm and BTM regarding the physics of the HDM. It will be the aim to show different influences to the inundation by different water levels with emphasis on changing determining factors which effect the inundation extend.

# 2 Methodology

## 2.1 Study area

This work is based on the study area of Kiel, the capital of the state Schleswig-Holstein in Germany. More precise the investigations were done on the inner Fjord of the city (Fig. 1). The data for the terrestrial DEM for the investigations are based on the amtliche topographische-kartographische Informationssystem (authoritative topographical-cartographical information system, ATKIS) catalogue which is a database for digital landscape models. It was generated by the State Surveying Authority of Schleswig-Holstein. The original resolution is 1x1m and displays the elevation of the land (Amtliches Topographisch-Kartographisches Informationssystem 2008). This basic data was provided by the Geographical Institute of the University of Kiel. The second part of the basic data for the DEM was the bathymetry of the Kiel Fjord. The measurement was carried out by the Bundesamt für Seeschifffahrt und Hydrographie (BSH; National Authority for maritime navigation and hydrography). It represents the depth of the water instead of the heights and has a general resolution of 30x30m. This data where provided directly by the BSH.

Generally Kiel lies at the south-west of the Baltic Sea. The region is certainly shaped in the Weichselian glacial period. The narrow and deep shape of the Fjord is related to erosion by glaciers and melt-waters. In the last 130 years anthropogenic modifications took place and influenced the shape essentially (Kögler & Ulrich 1985, pp. 1-3). The recent waterfront shows different highly frequented utilisations like harbours, tourism, shipyards, residences and catering. Nowadays the waterfront is characterised by long parts of sea walls and relatively high lying. Inundation events are relatively rare because of the elevation. For an inundation event particular trigging circumstances have to occur. For example northerly to easterly winds have to prevail in a strong manner to negligible tides, an inundation usually is a wind driven phenomenon. The most known threatening event was the storm surge from 1872, with a water level of 3.40m above MSL (Geckeler, Ynr).


Figure 1: Kiel Inner Fjord - Study-Area; Source: Top25, Landesvermessungsamt Schleswig-Holstein

## 2.2 Inundation scenario

The scenarios for the investigations were derived from an event of a relative high probability and, to create a theoretically future risk event, additionally SLR was taken into account. The deliberation was to choose an event which had on the one hand a high water level, but on the other hand also a high probability of occurrence. To figure out inundation areas at this study area, an event of relative high water levels had to be simulated to get inundated areas because the coastline of Kiel has relatively high altitude. A storm called Daisy from 2010 was chosen as basic hydro-meteorological event. It represents a common storm event for the area of the south western Baltic and had average values in respect of a storm in water level

heights and wind velocities. Water levels up to 1.5m were measured as maximum in the Baltic and the wind-regime was a north easterly of 7-8 Beaufort up to a violent storm (BSH 2013a, p. 1). The maximum difference to MSL for the gauge Kiel-Holtenau was 1.21m at 6:46 in the morning of the 10‘Th of January regarding the measurements. A small storm surge at the German Baltic coast is by definition of a height between 1-1.25m (BSH 2013b). This kind of event can be expected during the strong winter and spring storms every three to four years or even oftener. Defining a storm surge, it describes the time range of high water levels, but not only the maximum water level (MWL) itself. However the MWL is the indicating factor to classify the surge (Schumacher 2003, pp. 83-90; Schumacher 2003, p. 98). Due to the fact that most scenarios focus to the year 2100, the focus felt on predictions for this time. Down scaled models were generated on basis of emission scenarios and produced for the Baltic regionally different mean sea levels. Those models indicated the risk will be highest in future climate for the eastern and southern parts of the Baltic. A probable SLR of 33 -125 cm by 2100 which is in average 75 cm (Graham 2008, pp. 197-198) is predicted. There is no overall agreement and obvious uncertainties, but this information was taken for the scenarios which should be the base for the MIKE21 and BTM investigations. Furthermore it was mentioned that extreme sea levels will increase significant more than the mean sea level due to changing wind regimes. But this will not be taken into account at this place, because of the increasing uncertainty and the increasing demand to validate the model further. Due to this information different scenarios were considered:

(a) Daisy as a stand-alone event with a maximum water level of 1.21m

(b) 0.33m as lowest SLR for the Baltic in addition to Daisy

(c) 1.25m as highest SLR for the Baltic in addition to Daisy

Because the main advantage of Hdm in respect to BTM is the physics, the advisement was done to run the scenarios with different surface resistances. As primary information Tab. 1 was used, where the different resistance coefficients were taken from (Kaiser 2011, p. 2525). The decision fell on a Manning coefficient M of 32 as default set-up in MIKE21. Further there were runs done with a Manning M of 17 as middle density urban area and 12.5 for high density urban area. Due to the limited information and time a further land cover classification was not carried out, so these values got assumed for the whole area. An additional improvement would be to classify for example each building and to generate, by using remote sensing, differentiated roughness maps. But this would exceed this work at the moment.

Table 1: Land-cover classes and relating Manning parameters; Source: Kaiser (2011), p. 2525

| Land cover class | Mannings $n$ | Manning $M$ in $m^{1/3} s^{-1}$ | Source |
|---|---|---|---|
| Barren land/mud, sand, beach, roads | 0.0310 | 32 | b |
| Grassland | 0.0360 | 28 | b |
| Young Plantation | 0.0370 | 27 | b |
| Scrubland | 0.0380 | 26 | b |
| Cashew Plantation | 0.0430 | 23 | b |
| Other plantation | 0.0430 | 23 | b |
| Coconut plantation | 0.0458 | 22 | a |
| Semi open landscape | 0.0550 | 18 | b |
| Oil plantation | 0.0573 | 17 | a |
| Middle density urban area | 0.0600 | 17 | c,d |
| Melaleuca forest | 0.0550 | 18 | b |
| Rubber plantation | 0.0609 | 16 | a |
| Casuarina forest | 0.0731 | 14 | a |
| Inner beach forest | 0.0744 | 13 | a |
| High density urban area | 0.0800 | 12.5 | c,d |
| Other forest/rainforest | 0.0850 | 12 | c,e |
| Outer beach forest | 0.0870 | 12 | a |
| Mangrove forest | 0.0951 | 11 | a |
| Buildings non-resistant | 0.0900 | 11 | c,f |
| Buildings resistant | 0.4000 | 2.5 | c,f |
| Mangrove area 2005 (post-tsunami) | | | |
| Mangrove → water | 0.0110 | 90 | a,b,g |
| Mangrove → mud | 0.0310 | 32 | a,b,g |
| Mangrove → damaged understory | 0.0310 | 32 | a,b,g |
| Mangrove → sand | 0.0310 | 32 | a,b,g |
| Mangrove → inclined, roots remaining | 0.0360 | 28 | a,b,g |
| Mangrove → no damage | 0.0951 | 11 | a,b,g |
| Mangrove → indirect damage | 0.0951 | 11 | a,b,g |

Values are derived from [a] measurement of tree stand parameters in the field followed by calculation of Manning's n according to Eq. (1); [b] measurement of stand parameters for different land cover classes in the field and subsequent estimation of Manning's $n$; [c] literature; [d] Kotani (1998) in Latief and Hadi (2007); [e] Arcement and Schneider (1989); [f] Gayer et al. (2010), Leschka et al. (2009); [g] + change detection/Ikonos

## 2.3 Digital elevation model

The main important data for this kind of environmental, spatial analysis is the "Digital Elevation Model" (DEM). Both approaches mentioned in the introduction are limited by the spatial resolution of the DEM (Van de Sand et al. 2012, p. 569). A DEM is a digital, quantitative representation of the earth‘s surface. It includes and provides basic information about the terrain. Parameters like slope, drainage area and topographic index are important for every kind of environmental modelling and assessment. For example, they determine how much water discharge a river has, conditioned by the slope and drainage area. Different techniques such as photogrammetry, interferometry or airborne laser scanning are applied to generate DEMs (Mukherjee 2013, p. 205).

The limitations of spatial approaches using a DEM are caused by different resolutions of the generating techniques. There are public available DEMs like Aster GDEM (Advanced Space¬borne Thermal Emission and Reflection Radiometer) or SRTM DEM (Shuttle Radar Topography Mission). The Aster has a resolution of 30x30m; SRTM has 90x90m (Van de Sand et al. 2012, p. 570). In comparison LIDAR (Light Detection And Ranging), which is the airborne laser scanning technique, can resolve up to a nominal point density of 2 points/m². It is obvious that analysis with data of higher resolution lead to more extensive results. But also a higher resolution causes a higher amount of data, which affects a higher demand of

computer memory capacity. A higher data density also requires a higher amount of computing capacities to get results in an acceptable amount of time.

Following Wainwright and Mulligan, "something is complex if it contains a great deal of information that has a high utility, while something that contains a lot useless or meaningless information is simply complicated“ (Wainwright & Mulligan 2004, p. 2). It should be the aim to make problems complex rather than complicated. The optimal model is the one that contains sufficient information, but not more. “Any approaches, whether it is a qualitative description or a numerical simulation, is the try to achieve this aim“ (Wainwright & Mulligan 2004, p. 2). Therefor the resolution of a DEM should be functional in respect to the question of investigation.

However, those data measured are set into a 3-dimensional coordinate system. Due to support of global positioning systems (GPS) every measured value of altitude, which are the z-values, gets coordinates in “x“ and “y“ direction. In result it is a “.xyz“ file which gets further processed to a DEM. What kind of format this x and y values are transformed to, depends on the definition of the reference datum and coordinate-system. Due to the fact that most of the measurements are made supported by GPS the common datum is the World Geodetic System 1984 (WGS84) which the datum GPS is based on. The elevation of a point of the local earth surface in respect to mean sea level (MSL) can vary to the elevation computed by GPS. The GPS coordinates are computed on basis of the WGS84 ellipsoid. The earth instead is the geoid, what can result in differences in elevation between geoid and ellipsoid. “The geoid surface is an equipotential or constant geo-potential surface which corresponds to mean sea level. The geoid height/geoid undulation (N) is the difference in height between geoid and ellipsoid at a point“ (Mukherjee 2013, p. 206). However it can be derived that: h = H + N where is: h = represented ellipsoid height, H = height above geoid surface, N = geoid height, see Fig. 2 (Mukherjee 2013, p. 206). This means GPS could overestimate the real height depending on localities.

The two following examples show, how these data look like when taken and written by the measuring systems and how they look after processing. In Fig. 3 every line represents one coordinate point. The first column is the x, the second column the y and the third column the height, the z coordinate. If all points are computed the result can look like Fig. 4. Depending on the resolution (point density of the measurements) the DEM gain or loses extent. The example in Fig. 4 represents a DEM of Kiel. Like mentioned above the generation of this basic data is an essential part of getting information about inundation.

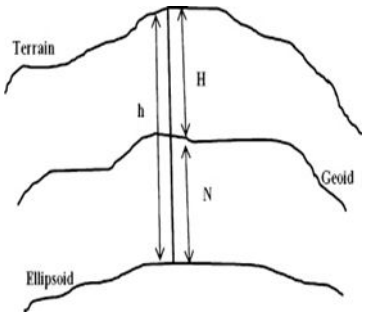


Figure 2: Differences between geoid and ellipsoid; Source: Mukherjee (2013), p. 206

3570000 6019040 11.03

3570005 6019040 10.95

3570010 6019040 10.82

3570015 6019040 10.85

3570020 6019040 10.88

3570025 6019040 10.89

3570030 6019040 10.90

3570035 6019040 10.92

3570040 6019040 10.94

Figure 3: Example of an output “xyz-file“ from a DEM measurement

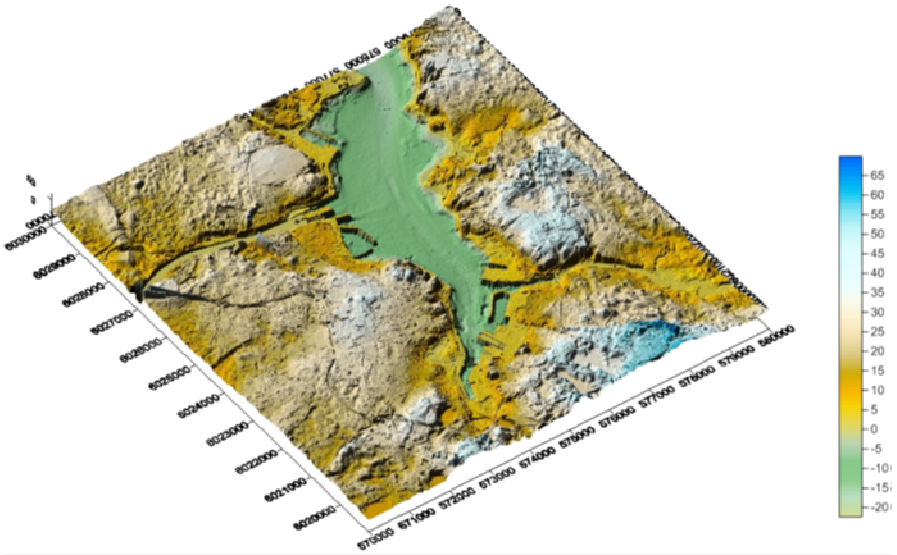

Figure 4: Generating the DEM : Example of a “xyz“ file after processing, resolution 10X10m

## 2.4 Preprocessing

The land and water area data set have to be combined to get one homogenous DEM for the land side as well as for the water area. The DEM data were airborne generated, measurements of the water area were taken by sonar. The ATKIS DEM had to be “cleaned“ from values of the water area with the effect of having no more information of the DEM in the Fjord. Otherwise these areas would provide errors when interpolating. This was done within ArcGIS by creating a polygon of the coastline and deleting everything within it. The corrected DEM of Kiel became the basis for the BTM investigation later on.

Both datasets are ASCII file which further became processed by the editor software TextPad. It has the ability to work in columns and rows within ASCII files, so both datasets were brought together, adjusted and formatted to a conform shape. Before processing further it had to be considered which area of the Fjord was of interest, for what a list of three decision guidance points were constructed:

- The area should be as small as it was practical for an inundation simulation; to minimise computation demands

- The area should show a distinctly inundation in the web-GIS of the city Kiel to increase the probability of inundation while Hdm (because of expectation of less inundation in modelling approach due to physical interactions)
- The area should be of a certain economic interest (for eventually further investigations like vulnerability assessment)

The coordinates of the Inner Kiel Fjord are:

Lower left corner: 3573400 x-direct. / 6020400 y-direct.

Lower right corner: 3577500 x-direct. / 6020400 y-direct

Upper left corner: 3573400 x-direct. / 6024040 y-direct

Upper right corner: 3577500 x-direct. / 6024040 y-direct

After pre-processing a complete ASCII file was created as a .xyz file for the area of interest (AOI). The further processing went on with interpolating the joined data due to the fact that both basic data had different resolutions. To get homogenous resolved DEM software for contouring and 3D surface mapping, called Surfer by Golden Software was used. Using this software it was enabled to generate a controlled grid with acknowledge of the background geo-statistics. Within Surfer kriging was described as a flexible method to generate good griding results (Golden Software 2002, p. 117). In Surfer kriging can be used as interpolator which “incorporates anisotropy and underlying trends in an efficient and natural manner“ (Golden Software 2002, p. 117). Anisotropy describes the equality of a parameter in a direction compared to another one. To give an example, imagine a shoreline where the probability of equal sediment parallel to the shoreline is more likely as perpendicular to it (Golden Software 2002, pp. 108-109). Because there was anisotropy due to the two different densities in the datasets it was decided to use kriging. To get an overview about the spatial distribution, the spatial dependence of points to each other, as well to provide the needed information for interpolating the data by the kriging method, a variogram was produced (Fig. 5). Variogram are used to investigate how grid-points do relate to each other in the manner of spatial dependence. It shows how far a certain point has to be away from a central point, on which the measurement is based on, to be un-associated to it. In Fig. 5 the experimental variogram is displayed by the dots. A fitted model is shown as solid blue line, which is the function the kriging was based on for an interpolation. Beside visible in Fig. 6 is the plateauing of a variogram. The beginning of the plateauing is the distance where points are no longer associated to each other. It is the so called “range“.

As mentioned above, that information are needed to ensure a reasonable interpolation when the kriging method is used (Harris, R. & Jarvis, C. 2011, p. 209).

The key behind this concept is to calculate the variance as a function of the distance away from a central point. This is computed for each point to every other one in the data set. The calculated variance values are assigned in so called “lags“ which are sections of distances from zero to the maximum measurement of distance. The maximum measurement of distance is equal to the maximum search radius from a central point, to points which are gone to be compared in terms of variance. The measured variance in dependency to the distance can be plotted as an experimental variogram, shown in Fig. 5 (black line with dots).

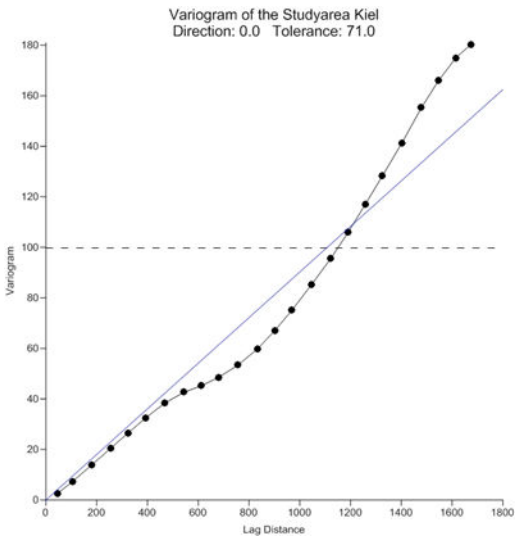


Figure 5: Variogram of the Study area produced with Surfer

Further there are general rules of thumbs for the construction of a variogram. The first one is that at least 50-100 points are needed to generate a variogram, this is case depended due to the variation in the amount of data points in each lag. The data set for the variogram of the study area has an absolute number of 124280 points. The second one is the maximum lag distance should be less than half the wide of the study area (Harris, R. & Jarvis, C. 2011, p. 210-211). In this study the AOI is 4100 meter wide. Surfer uses this information and produces a max lag distance (MLD) by default which is less the half wide (shown in Fig. 5; half wide 2050, Surfer produced MLD 1800). The most conspicuous is that there is no plateau. This means every point is associated with each other point within the maximum distance of searching. Another point to recognise is the curve itself. Due to the fact there is no plateau, the curve ascends continuous. This is caused of the relative high point density in the DEM as therefor a high dependency between the points. It is likely that the variations of the experimental variogram are little because of the different point densities of the topography and bathymetry. To get the variogram function (blue line in Fig. 5) which is used further as the function for interpolating, Surfer includes a range of so called models to describe the experimental variogram. The best fitting should be used to result in a reasonable function for the interpolation. Due to the fact the curve is nearly linear, the linear model was chosen. By the option AutoFit within Surfer the linear model got a slope of 0.059, anisotropy of 2, and an anisotropy-angle of 40.59, which is also caused by the lower point density of the bathymetry in the Fjord. Due to the acceptable fitting of the variogram model, the resulting grid after the kriging interpolation was considered to be reasonable and was used for the further modelling investigations. However, also the nearest neighbour interpolation was used to produce a surface, to compare the results of the kriging and the nearest neighbour interpolation (shown in Fig. 7). By comparing the different results visually, the nearest neighbour surface shows a rougher structure than the kriging result, especially in the water area. Those unrealistic irregularities strengthen the relevance of the kriging grid. The pre-processing was finished at this point.

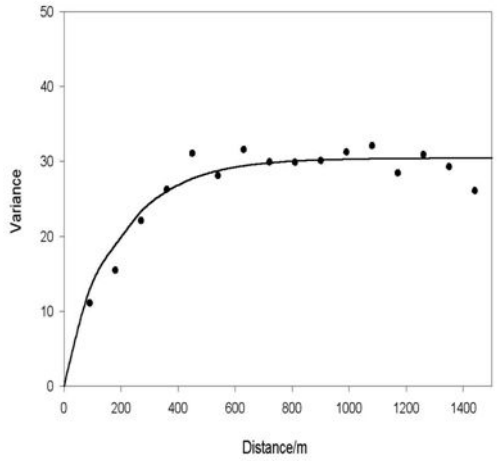


Figure 6: Variogram of the residuals from the trend for elevation; Source: Oliver, M.A. & A.L. Kharyat, (1999)

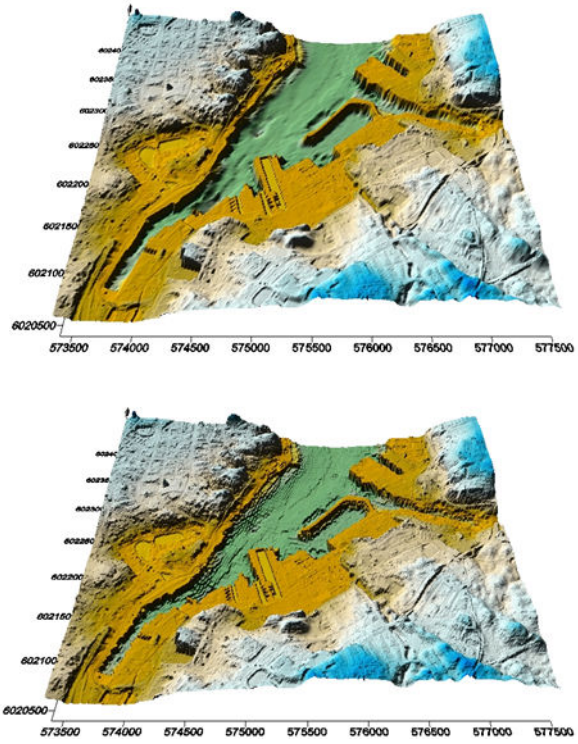


Figure 7: Upper surface represents the kriging, lower surface shows nearest neighbour calculation

The following Tab. 2 gives an overview of the working steps in general. It represents the different steps which had to be processed to generate inundation maps of the three scenarios for the study area and to calculate the inundation statistics.

Table 2: Workflow

| Working step | Software tool | Needed Data |
|---|---|---|
| 1. Clean original DEM from water values | ArcGIS 10.0 | • ATKIS DEM 10x10m<br>• Coastline Kiel |
| 2. Merge DEM and bathymetry data, bring it to uniform shape | TextPad | • Corresponding ASCII files |
| 3. Generate Variogram | Surfer 8 | • Merged ASCII file |
| 4. Interpolate ASCII file and generate grid | Surfer 8 | • Merged ASCII file<br>• calculated variogram |
| 5. Validating MIKE21 | MIKE21 | Time series of gauge:<br>• Kiel/Holtenau<br>• Geomar<br>Time series Wind:<br>• Lighthouse/Kiel<br>• Generated grid |
| 6. Setting up proper SLR scenarios and controlling a satisfying implementation | MIKE21 | Time series of gauge:<br>• Kiel/Holtenau<br>• Literature |
| 7. Generate BTM inundation maps (see 3.4 applying the two approaches) | ArcGIS 10.0 | • Generated grid<br>• Shape file of the Fjord<br>• Scenarios |
| 8. Run simulations on different scenarios (see scenarios in 3.3 Inundation Scenarios ) | MIKE21 | Time series of gauge:<br>• Kiel/Holtenau<br>• Generated grid<br>• Land-cover roughness classification values<br>• Scenarios |
| 9. Surface analysis | ArcGIS 10.0 | • Simulated grid files from MIKE21<br>• Inundation areas from BTM analysis |
| 10. Presenting the results | ArcGIS 10.0 | • Surface statistics |

## 2.5 “Bathhub” inundation approach

The following part describes how ArcGIS 10.0 was used to generate inundation maps for the "Bathtub Method". The key behind this method was elucidated in the introduction above; regarding this the following section will deal with the application on the study area. Like mentioned in the section 2.4 Pre-processing the in Surfer generated grid was the base for further investigations and the first step of applying any approach. The second step was to convert a shape file of the water area, which was a part of the ATKIS catalogue, to a raster with cell sizes accordingly to the cell size of the DEM. This was done by Conversion Tools -To Raster -Polygon to Raster. The next step was to create a mask out of this new raster. Therefor the raster had to be reclassified. This was done by Spatial Analyst Tools -Reclass -Reclassify. The aim was to change the value of the water areas to zero and anything else to one. So that in the fourth step the DEM values got multiplied by one and the water became the value zero. The result was a corrected surface, where the water became zero as a base-level and the land got its correct elevation. This step was fulfilled by the help of the tool "Raster Calculator". Within "Raster Calculator" the statement “Con(,)“ was used to define a condition. Basically the condition was, if the pixel value of the raster is zero, than the new value will be zero otherwise the pixel will get the value of the DEM for this coordinate. The fifth step was to generate the inundation area itself. Therefor again the "Reclassifying" was used that way, the values from zero to a certain value (max water level) were classified as zero and any value above was classified as one. The result was a two coloured map, showing the land and the inundation. To become more accurately "Region Group" was used in the next step to filter out the hydrological connected areas. Following Cooper et al. (2013), they also carried out a BTM analysis for Maui, Hawaii with the aim to get a quantitatively

assess of the spatial distribution of inundation. Therefor they reclassified their DEM by the given heights of the regional expected scenarios. Different to Rodriguez (2010) they separated vulnerable areas in hydrological connected (HC) and disconnected (HDC). Areas of HDC were mapped separately to take them into account for a “complete-as-possible“ analysis. Due to the problem of uncertainties in vertical accuracy, they calibrated and validated the DEM on different tidal benchmarks. The reference for the tidal benchmarks was MSL. Further they took local specification on the tide regime into account, in this case a semidiurnal tide with a Mean Highest High Water (MHHW). In their further investigations they produced 8 GIS vulnerability layers. They distinguished by HC plus basic DEM, HC plus corrected DEM, HDC plus basic DEM and HDC plus corrected DEM. The results are shown in Fig. 8. Those high resolution vulnerability maps are important to identify low lying coastal areas. They highlight the critical need to act and improve community resiliency to climate change.

To take this into the here applied approach, within "Region Group" some set-ups had to be considered. So the number of neighbours had to be eight, the zone grouping should be set as “within“ and the “Add link field“ button had to be deactivated. This was done to get pixels which are also connected diagonal additionally to the ones which were connected on the sides (Cooper 2013, pp. 554-555). Now having the hydrological connected areas, the raster had to be reclassified again the way how it was done in the fifth step, again with an inundation value of zero to the certain scenario level. In the end the results were hydro-connected areas of an inundation for a certain scenario. At last there was the interest in numerically precise information about the areas which were inundated. Therefor the former generated polygon of the Fjord, which was created to correct the original DEM and to delete the values of the water while pre-processing, was used. This polygon was further modified by the areas of the "Kiel-pond", the "old boat-harbour" and the "Schwentine river" inflow. This was done to subtract real water areas from the inundation areas. Without doing so, all water areas, even the Fjord itself, would be taken into account when calculating the real size of inundated land. In the end the displayed area of inundation had to be used as mask. By using "Spatial Analyst Tools -Extraction -Extract by mask" the wrought inundation areas were taken as mask to get the DEM of the corresponding area. This was necessary to get absolute values for the numerical analysis. But it has to bear in mind, inundation is not a stand-alone event. Moreover it is a result of different factors which can cause coastal hazardous events. The list starts at SLR, changes in mean wave height, tidal oscillations, changes in long shore currents, sediment transport, changes in wind direction and strength, rainfall and due to this flooding, change in vegetation and ends in geomorphology (Muthusankar 2013, p. 2402). Therefor the BTM can only be a way to identify exposed areas. While using BTM for this kind of problem all physics are neglected. Inundation is not just like the water level rises and floods a particular area. Hydrodynamics take place which are for example flows, currents and turbulences which can be caused by flushed obstacles. Also an important parameter during inundation is the resistance or friction. If water attains the land, its flux behaviour changed. Depending on the structure of the surface, fluxes can be slowed down more or less or can even block nearly completely (Kaiser 2011, p. 2522). Depending on these parameters the area of inundation is influenced. To get those parameters within analysis HDM were developed. Those models work on physical equations and compute designated parameters for every grid cell. The following part provide a basic understanding of the difference of a HDM to the BTM .

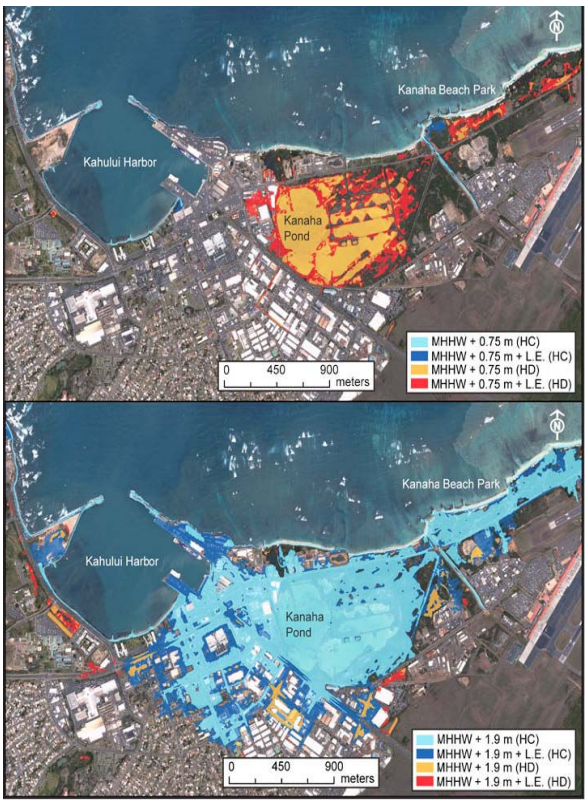


Figure 8: Results of Cooper et al. from their inundation investigation of Kahului Harbour Area, Hawaii; Source: Cooper (2013), p. 558

## 2.6 Hydrodynamic modelling approach

In this study the HDM MIKE21 by DHI (Danish Hydraulic Institute) is applied to model an inundation analysis for the study area of Kiel. MIKE21 is a complete software suite for modelling 2-Dimensional free-surface flows. It is applicable in nearly every coastal area to simulate hydrological and environmental phenomena. The hydrodynamic module is able to perform operations on the forcing of different driving effects such as wind shear stress, momentum dispersion, flooding and drying and wave radiation stress. It is mainly applied and developed to calculate tidal hydraulics, wind and wave induced currents as well to simulate storm surges and coastal flooding. MIKE21 is a universal HDM which also can be used to model dyke breaches, tsunamis or harbour seiching (DHI 2009, p. 13-14). It simulates unsteady 2-Dimensional flows in one layer. This means the water column is assumed as vertical homogenous (no differentiation in stratification, e.g. of density due to salinity and temperature). It works on the basis of the mass and momentum conservation in space and time. The numerical applications in MIKE21 HD (hydro dynamics) run on an alternating direction implicit technique to integrate those equations matrices, for each gridline in each direction. To give a simplified outlook about the physics which are behind the shallow water equations system SWE, it will be elucidated in the following section.

Following Raymond (Ynr) the SWE form a system to describe the behaviour of fluid flows. For its plainest form to understand, there were made some requirements which are assumed. The most important condition for the SWE to take effect is, that the horizontal scale of flow is large compared to the depth and the water surface has a weak slope. It is assumed that the water column has a uniform density ρ and the water layer has a thickness h (x,y,t). The water flows, in this simplification, over a flat ground so h is equal to the elevation of the surface. The velocity v is assumed to be independent of the depth v = v(x,y,t)

and nearly horizontal. Also to simplify, the bed resistance is neglected and the column is in hydrostatic balance. Therefor the pressure is uniform over the depth. Of course there can be a vertical flow factor due to bed elevation changes, but because this is an assumption it can be resolved by the continuity equation after solving the SWE. In general it is a system of three equations which are derived from the Navier-Stoke equation. The Navier-Stoke equation is the general equation to describe fluxes and is derived from Newton's laws, particular the mass and momentum conservation. The SWE fundamental three parts are the:

1. hydrostatic equation
2. momentum equation
3. mass conservation

The hydrostatic equation is: $dp/dz=g\rho$ (1.1)

The pressure p over the depth z is equal to the gravity acceleration g times the density ρ. Because the column is homogenous we can integrate over the depth as: p=gaze (1.2). The pressure p is equal to gravitation g times density ρ times the depth z.

This is the first equation which has to be noted. Due to this averaging the problem becomes two-dimensional and the vertical dimension is no longer of interest.

To derive the momentum equation and in this the second fundamental part it is needed to generate the horizontal pressure gradient. The operator becomes 2-D when $\nabla = (\partial/\partial x, \partial/\partial y)$.

From equation (1.2) we get $-\rho^{-1} \nabla p = -g\nabla$ (1.3). This is the horizontal pressure gradient per unit mass. It works as the pressure gradient in x and y direction at the surface and due to a homogenous column for the whole body. The operator is nothing else than the split pressure gradient in x and y direction which derives from the density. Simplified this means that the pressure gradient derives from the height of the water column accelerated by the gravity. Further there has the Coriolis force to be considered. The Coriolis force per unit mass is $-2\Omega x v$ (1.4) because the vertical component is small in comparison to pressure gradient and gravitational force it will be neglected. For neglecting this component the Coriolis force has to be split up in horizontal and vertical components. Therefor we resolve $\Omega=\Omega_h+\Omega_z z$ into its two parts. So the Coriolis force is $-(2\Omega_h x v+2\Omega_z z x v)$ where the first part represents the vertical component (h for height in vertical direction) which will be again neglected. Resulting in the so called Coriolis parameter, which will be further used, is named $f=2\Omega_z=2I\Omega I \sin\Phi$ where $\Phi$ is the angle of latitude. The retained part is thus $-fzxv$ combined with the pressure gradient force the momentum equation is obtained from Newton's second Law as:

$$\frac{dv}{dt} + g\nabla h + fz \times v \quad (1.5)$$

This means that the velocity v over the time t derives from the pressure gradient force plus horizontal Coriolis parameter. At a given time t the velocity is as high as the pressure gradient and the Coriolis parameter enable it to be. Because the column is homogenous this can be assumed over the depth. It is the second fundamental part of the SWE system.

The third key point is the mass conversation therefore we will use a sketch as example. Imagine the water column in the sketch (Fig. 9) is a cuboid of the side length L. Simplified the time rate of changing the volume is equal to the net inflow from both sides x and y.

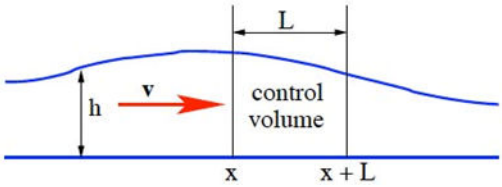


Figure 9: Sketch of the control volume for the mass conservation, Source: Raymond (Ynr)

Therefor it can be said:

$$\frac{dM_{cv}}{dt} = \rho L[\underbrace{h(x)v_x(x)}_{L_1} - \underbrace{h(x+L)v_x(x+L)}_{L_2} + h(y)v_y(y) - h(y+L)v_y(y+L)] \quad (1.6)$$

Simplified it could also be written:

$$\frac{dM_{cv}}{dt} = inflow_x + inflow_y$$

This is not correct but a plain description of equation (1.6) to get a notion. The change of mass of the control volume in Fig. 9 is equal to: the density ρ times the side length L multiplied by the product of the height h and velocity in x direction for the length $L_1$ subtracted from the product of height h and the velocity component in x direction over the Length $L_2$ plus the same operation for the y direction. In result this will give the velocity in x and y direction of the cuboid. $L_1$ and $L_2$ were defined to distinguish between those two lengths for calculating the absolute length of the variable for the cuboid.

Actually the term can be split in two major parts:

$$\underbrace{x}_{stands\ for\ L_1} \quad - \quad \underbrace{x+L}_{stands\ for\ L_2}$$

It refers to Fig. 9, the first term is the area left of the vertical x-line which has to be subtracted from the second term which is x+L. So in the result this makes the side length L. Further this part gives the components of the height by h and the velocity of flow in x and y direction by the indices vx and vy. Because the mass in the control volume can be written as mcv = ρ L h, when contributing the term of velocity in x and y direction this will lead to mass change. Due to mass change is a function over time, the changing rate is depending on the velocities.

In MIKE21 HD the equations of mass and momentum conservation integrated over the depth are used to calculate the flow behaviour and water levels (DHI 2009a, p. 11). Like described in the previous section, these are the fundamentals of HDMs. Within MIKE21 there are additional terms which work e.g. under consideration of resistance and stress factors and also varying bed structures. Further it is the aim of this short depiction to give a notion in which way MIKE21 uses these equations and solves the problems on a grid input file. The former elucidated equations get inputs like time series of water level changes or wind. Those inputs are files which are added to the model. The algorithm behind MIKE21 is a so called Double Sweep algorithm, which solves the equation matrices for every grid line in each direction at every time step n with the corresponding input-data. Those operating sweeps are alternating between x and y direction. Generally the so called x-sweep solves the continuity and mass equation for the x component. For terms which involve the y direction it uses the known old values from the y sweep operated before. Obviously at the beginning there are some conflicts within the corners of a grid but this problem will not be elucidated at this point.

The y-sweep solves the continuity and mass equation for the y direction, while terms involve the x component use the values just calculated in the x-sweep before. The system runs in an order of:

1. x-sweep decreasing y
2. y-sweep decreasing x
3. y-sweep increasing x
4. x-sweep increasing y

The first two are so called “down“ sweeps, the second two are so called “up“ sweeps. Those two groups alternate between the time steps. At a time step n the down sweeps in x and y direction operates until the whole grid is processed. Afterwards the up sweep start at time step n +1. Like it is shown in Fig. 10 the down sweeps start at the upper right corner and the up sweeps at lower left. After processing one x and one y sweep these are added together to get the calculation time centred. This happens because the different operations take a different amount of time. In the example in Fig. 10 the time centring is given at n+1/2. This is an immense important point because it is responsible for the stability of the model (DHI 2009a, pp. 9-15). For running MIKE21 HD the above shown surface of the kriging interpolation was used as grid to represent the study area. The calibration and validation was done by measurements of the event called Emma in 2008, data taken by: Wasser-und Schifffahrtsverwaltung des Bundes (Federal waterways and shipping administration), provided by the Bundesanstalt für Gewässerkunde (BFG; Federal administration for hydrology; Maritime Meteorologie, GEOMAR Helmholtz-Zentrum für Ozeanforschung Kiel). The so called “driver“, which represents the boundary condition was the gauge of Kiel-Holtenau (blue dot in Fig. 12). The other gauge for testing the quality of the MIKE21 calculation was a measurement at the pier of the Geomar Institute (green dot in Fig. 12). The idea for validating came from Remya (2012) and was to generate a curve of the water level change (WLC) by the calculation of MIKE21 at the position of the gauge at the Geomar. To sum up the validation, it can be described as the gauge at Kiel-Holtenau drives the model and is the primary force on which the kinematic of the model is based on (Remya 2012, p.387). At the green dot in Fig. 12 there has a virtual measurement taken place to generate a time series. At the end, the calculated time series got compared with the in-situ measurements to estimate how reasonable the models calculations are. It is a common manner to validated 2-Dimensional HDMs by point measurements of the water level change, flow velocity or flow direction measurements (Bates et. al. 2005, p. 798). But even this is a common application this is just a minimum of validation (Sutherland 2004, p. 121). Even more it has to be considered to make a wide distributed validation for coastal-shoreline management issues. While a point validation can show a reasonable accuracy, an inundation assessment needs in best case a validation for the whole area (Bates et. al. 2005, p. 798). Because the shoreline of Kiel is generally relatively high lying and the local hydrodynamic regime of the Baltic is not that threatening in case of storm surges for the inner Fjord, there are no information about surveys of inundation or maps of earlier flood events provided by the authorities. Due to this lack of information the only way of validating was the comparison of this WLC time series with the calculated one. Like described in Remya (2012) they focused on e.g. wave height and wave period for their performance evaluation (Remya 2012, p. 387). In this case it was water level change because of the limited information. Fig. 13 presents the calculated water level change over the time. The red line is the in-situ measurement of the gauge at the Geomar Institute, the blue line is the water level change of

gauge Kiel-Holtenau and the green line is the MIKE21 calculated time series for the position of the Geomar gauge.

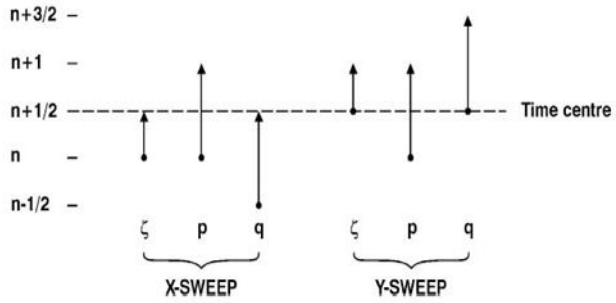


Figure 10: Time centering between x and y sweep; Source: DHI (2009a)

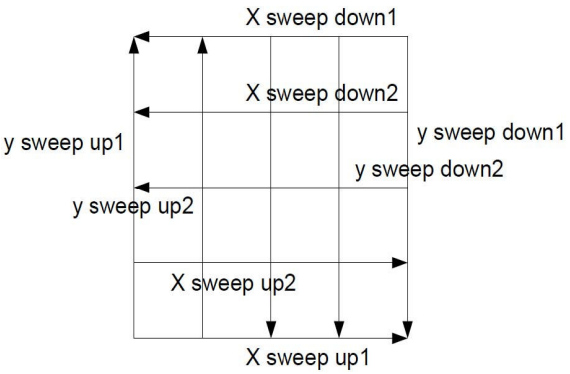


Figure 11: Order of calculating sweeps

Starting with some uncertainties at the beginning the calculated curve comes to a smooth fitting between the driver curve of Kiel-Holtenau and the validation curve of the Geomar. Apparently the calculated curve over-predict at the peaks in comparison to the in-situ Geomar curve. A calibration was fulfilled by changing wind parameters, and friction. Both applications didn't have had influence on the validation results. All further parameters within MIKE21 were set as default, as this was a basic application of the model.

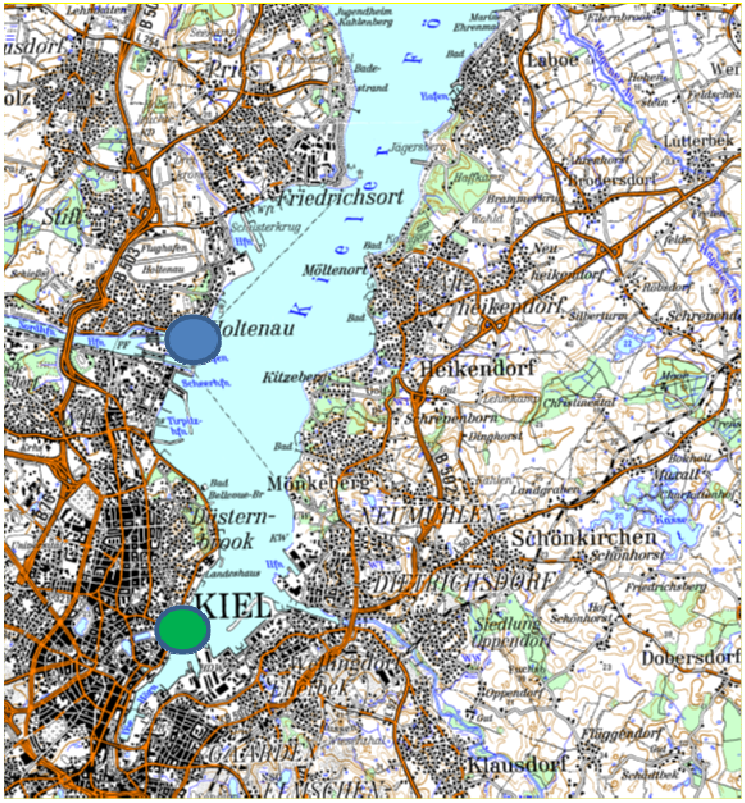


Figure12: Dots represent the water level gauges within the study area; Source: Top 25

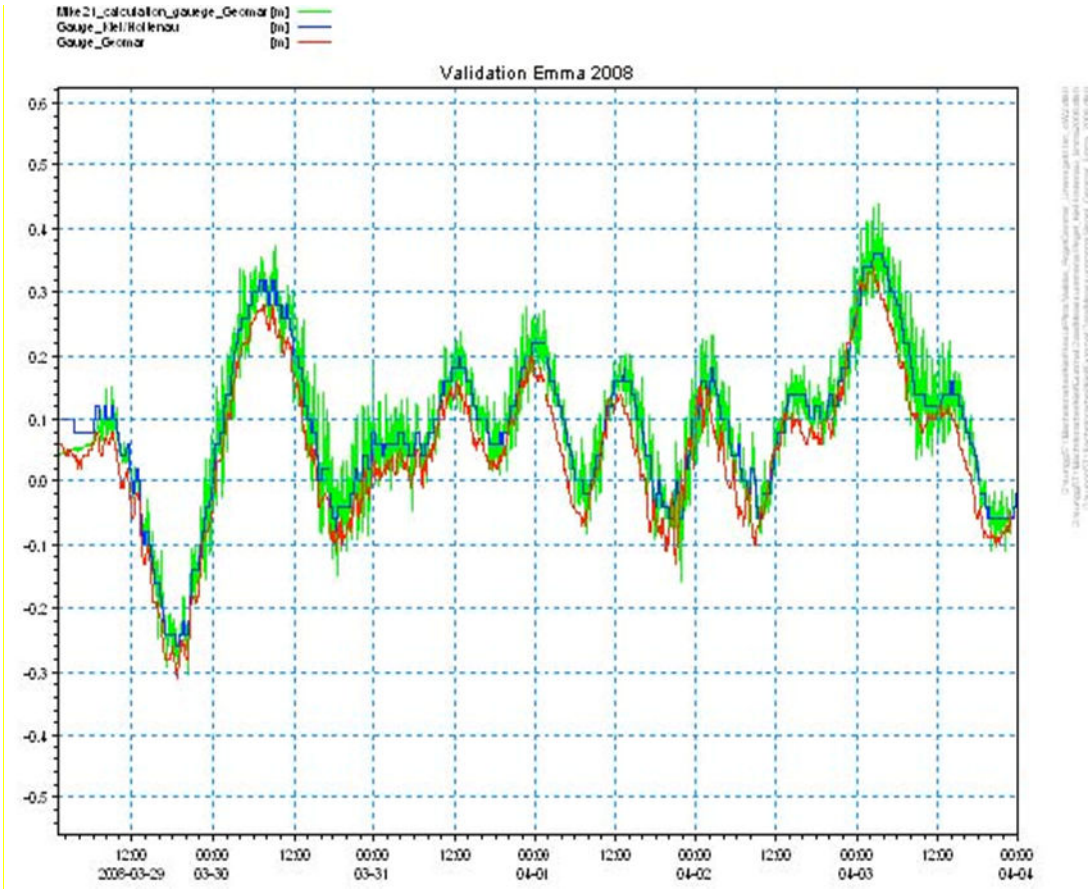


Figure 13: Validation of MIKE21 comparing to in-situ measurement at Geomar; derived by gauge Kiel-Holtenau

Following the graphical presentation, statistical results are needed to give a statement about the quality of the MIKE21 calculations. The used statistical parameters are the correlation coefficient, the bias, the average square of the difference, the average difference and the root mean square error. The following variables are explained as: m = modelled $\overline{m}$ = mean value of the model derived parameter, $\overline{obs}$ = mean of observed data and obs = observed data (Remya 2012, p. 389). The correlation coefficient is a tool to calculate, if two variables are significant related. It is presented in equation (2.1). It represents how consistent both variables change together, but bearing in mind that there has no blanket relation to be. The so called Pearson coefficient represents the linear correlation and can be a value between -1 and 1 where a result of +1 shows a perfect positive correlation. A negative coefficient results if the two variables behave contrary (McKillup & Darby Dyar 2010, pp. 194-196).

$$R = \frac{\Sigma(m - \overline{m})(obs - \overline{obs})}{\sqrt{\Sigma(m - \overline{m})^2 (obs - \overline{obs})^2}} \quad (2.1)$$

Another parameter, the Bias, represents the mean of all differences between the calculated and the measured numbers. It is shown in formula (2.2). The criticisms on this is, if a positive and a negative value get subtracted it may not reflect the actual size of the total difference. In result this means the value is not reliable to give an assessment of the models quality only based on this parameter. Furthermore the function of the "average square of the difference" should be used to get estimation about the actual mean difference between measured and modelled values, shown in equation (2.3). Due to the square negative values become positive but this is still, by definition, the "average squared difference" and gives the result in different units.

To get a reasonable idea about the average difference between the calculated and Geomar time series, it is recommendable to use the function of "average of the difference", shown as equation (2.4). By the square root the result gets the original unit and allows a reasonable reflection (Smith & Smith 2007, pp. 84-87). The RMSE (root-mean square error), equation (2.5), is often used to identify a relation between measured and calculated values. The RMSE results are in the same units like the original measurements. This makes it easy to interpret (Wainwright &mulligan 2004, p. 66). It is not identically to the average difference but because the values are of the same order, it provides an accurate comparison of the difference between a modelled and an observed time series. Representing the most accurate statistics it is one of the most important parameter to make a statement about the models quality (Smith & Smith 2007, pp. 84-87).

$$\text{Bias} = \frac{1}{n}\sum (m - \text{obs}) \quad (2.2)$$

$$\textit{Average of the difference} = \frac{\sum_{i=1}^{n} \sqrt{(m_i - \overline{o_i})^2}}{} \quad (2.3)$$

$$\textit{Average square of the Sum difference} = \frac{\sum_{i=1}^{n} (m_i - o_i)^2}{n} \quad (2.4)$$

$$\text{RMSE} = \sqrt{\frac{1}{n}\sum (m - \text{obs})^2} \quad (2.5)$$

The validation runs were set up once with and once without wind, but there were no differences in the calculated numbers. The effect of wind was negligible in this case due to the small fetch. Therefor the statistics of only one example are presented in the Tab. 3 which is the case of water level changes driven by Kiel-Holtenau. The general settings in MIKE21 were set to default with a Manning number of 32 and an Eddy viscosity of Smagorinsky

Formula of 0.5. The general results of validating the model are good and satisfying with a correlation of 0.929 and relative small differences in the remaining coefficients (see Tab. 3). Those results are interpreted as MIKE21 provides a good quality of simulating water level change rates for the study area, taken in mind this were done on the base of default settings. It will be assumed that also further investigations, which will be scenarios of rising sea level and storm surges as well as inundation of the study area, are generally of good manner.

Table 3: Statistics of the models quality

Validation Results of Mike 21 for Study Area Kiel

| Simulation/Parameter | Correlation coeffecient | Bias | Root mean square error | Average size of the difference | Average square of the sum of differences |
|---|---|---|---|---|---|
| Val_gauge_Geomar_aW | 0.929 | 0.036 | 0.0587 | 0.047 | 0.00345 |

The inspected hydro-meteorological event for this validation was chosen on the basis of notices from media and because these dates were the latest available data by the Geomar Institute measurements. The further investigation will take place on the data of the storm event called Daisy in 2010. This event was much more threatening in terms of water levels and so it is much more suitable to simulate a future inundation event to reach more extensive water levels.

Applying MIKE21 for the above formulated scenarios it starts again by using the generated grid from Surfer. After pre-processing the grid, it had to be exported as a xyz file. In MIKE21 the first step was to generate a bathymetry with the tool "Bathymetries" in the module MIKEZero. A certain work area had to be defined, which was done by specifying the coordinates of the lower left corner and defining the map projection as Non-UTM to generate an output which could be further processed in ArcGIS. Within the tool, the correlated xyz file had to be imported by using the "Background Management". To guarantee a proper import, the data type window had to be changed to .xyz file, afterwards the correct file had to be chosen and at last the right coordinate-system had to be chosen in the window „Convert from:“. Doing so imports the grid, which afterwards has to be imported from the background by using the corresponding button. The whole area had to be selected. Afterwards the "Background Management" was used to define the grids itself again. The right projection should be given, just the grid spacing have to be adjusted. If the grid dimensions do not change it self, by adjusting the grid spacing, divide the areas width and length by the grid spacing. The other set-ups were set as default, like for example the land value. After selecting "ok", it has to be interpolated. In this case it is not a real interpolation, rather than a conversion from points into grid cells. Afterwards the result is the now ready grid which can be used in MIKE21. But only having a bathymetry does not suffice to run a simulation. To run the model, drivers are needed, at least a water level change. In this case water level change and wind measurements were provided. These are time series which were generate by measurement system and had to be converted to a MIKE time series. This was done by importing them from an ASCII file by using the tool „Time Series“ or by editing a blank files and paste the values into the created column. After all data files needed for the modelling the actual model was set up. Therefor a new file was opened and the MIKE21 HD Flow model module was chosen. All calculations were done by a simulation period from the 08.01.2010 12:00:00 to 10.01.2010 13:00:00. The Set-up was set to 70560 time steps and an interval of 2.5 sec with a resulting max. Courant number of 7.46993. The Courant number is a parameter which describes the relation between flow or water level change celerity and the computational speed in the grid and describes how many grid cells the information moves in one time step. It should not be greater than 8, otherwise the calculation can abort (DHI 2009b, p. 74). The other parameters within the basic parameters were set as default except

the parameters "Flood and Dry". This was set as drying depth: 0.05m and flooding depth: 0.1m. Those two parameters determine at what depth dry land is taken out of the calculation (drying depth) and at what water level (flooding depth) the grid cell is taken into the calculation. The parameter "Initial Surface Elevation" depends on the water level which is given by the time series of Daisy. Further there where a set-up at for the parameter "Boundary". At the open boundary the time series of water level mentioned above of the gauge Kiel-Holtenau for the Daisy event was used. All further parameters were set as default, especially the "Eddy Viscosity" and the "Resistance". The "Eddy Viscosity" was given as Smagorinsky Formula and had a constant value of 0.5. For the first run the "Resistance" was given as Manning number with a constant value of 32. These settings were equal to the setting from the validation run. The last parameter which was user specified was the "Wind Conditions" which got the measurements from Kiel-Lighthouse. To get the SLR of the scenarios into account the DEM had to be modified. Therefor the DEM got subtracted by the corresponding different value of the scenario, what is done in MIKE21 by the tool "GridEditor". In result there were three different DEMs one with the true elevation, one with 0.33m less and one with 1.25m less. Every DEM was run with the Daisy event. Also to point out differences in the physical flux behaviour different resistance numbers were applied. To investigate the above formulated questions, of how the physics, in particular resistance, affect the inundation extend, every scenario was run with the different Manning numbers mentioned in the section 2.2 inundation scenarios. As next a test was made to see the quality of the simulation. Therefor a random point within the area of the Fjord was selected and a time series was extracted. The idea behind this was to compare the calculated time series with the gauge time series. A related oscillation of the two graphs were expected and would reveal a, on the input data, correct working calculation.

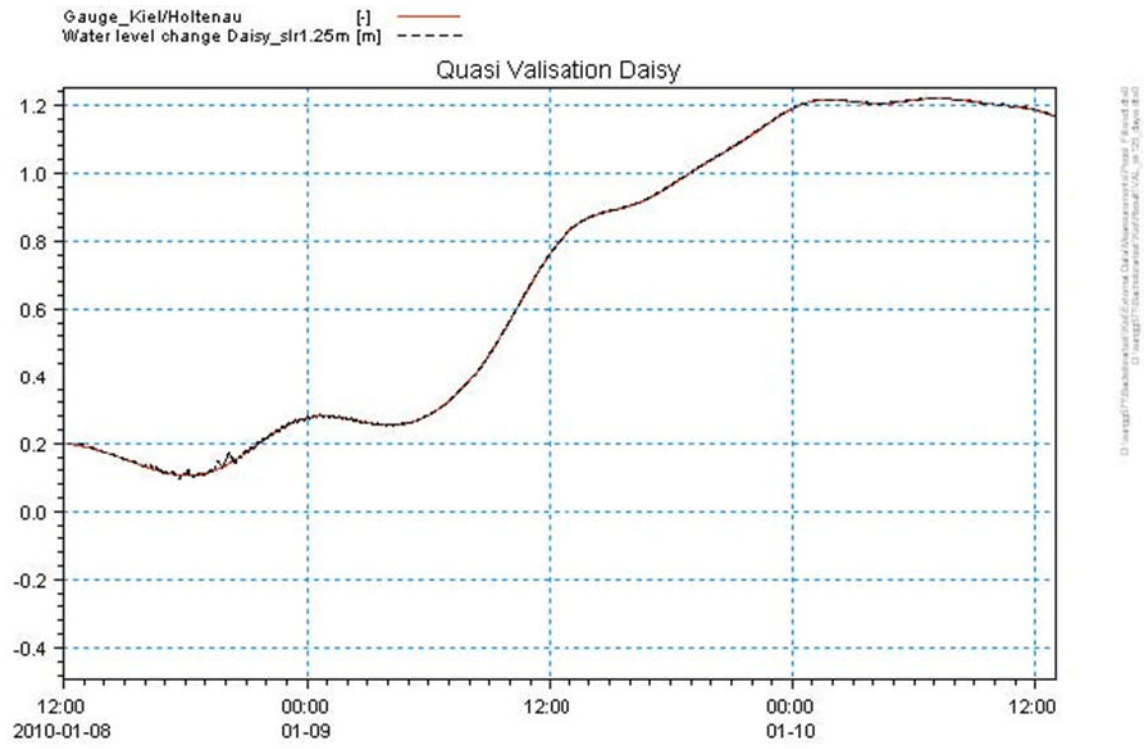


Figure 14: “Quasi calibration“ of MIKE21 calculating Daisy proper

Depending on the required problems or the case of investigation, calibrations can be done to different areas with differentiated resistance or e.g. if there are also time series of the wave-climate provided, these can be taken into account to the calculation. This is one of the differences of Hdm compared to BTM. There is a bandwidth of calibration possibilities to

specialise the model to the case study. Because it is not a core of this work to describe how to set up the model exactly, this documentation is pursuant short. For further information about how to set up a simulation in MIKE21 HD Flow model, please see the Step-by-Step user guide. After the calculation in MIKE21 was done, the results were exported by using the tool "MIKE2Grid". This produces an ASCII file which is readable by ArcGIS. Importing this file and rearrange the classes produces the inundation map of MIKE21 (Fig. 18-20). The further process is the same than in the BTM. So the real water areas had to be deleted, and the displayed inundation areas had to be taken as mask to extract the DEM for these areas, to calculate the statistics.

# 3 Results

The results which are here presented are the inundation maps and statistical results of the BTM and MIKE21 approaches. Following the graphical presentation, a statistical evaluation of the inundated surface area and of the volume of water which inundates will be presented. Starting with the presentation of the three scenarios Daisy without SLR, Daisy plus 0.33m SLR and Daisy plus 1.25m SLR of the BTM approach, the MIKE21 results will follow afterwards. The red coloured areas display the area of inundation.

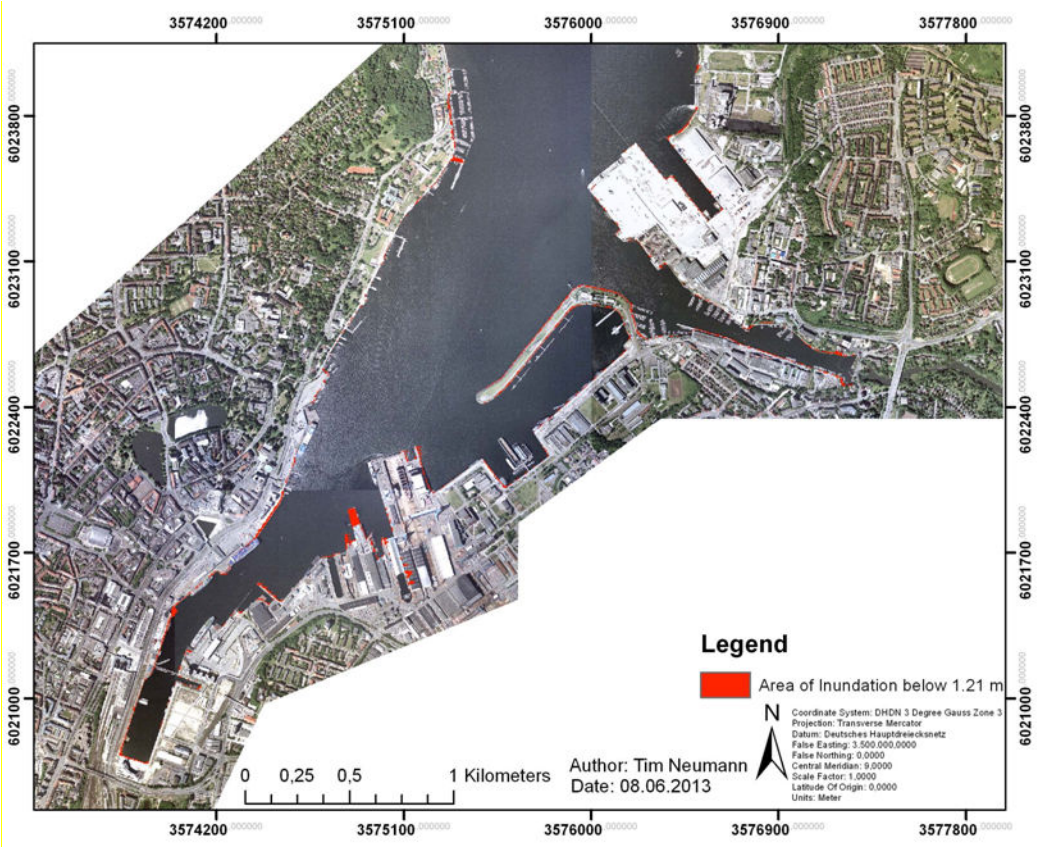


Figure 15: Inundation of Daisy without SLR. Maximum Water Level (MWL): 1.21m

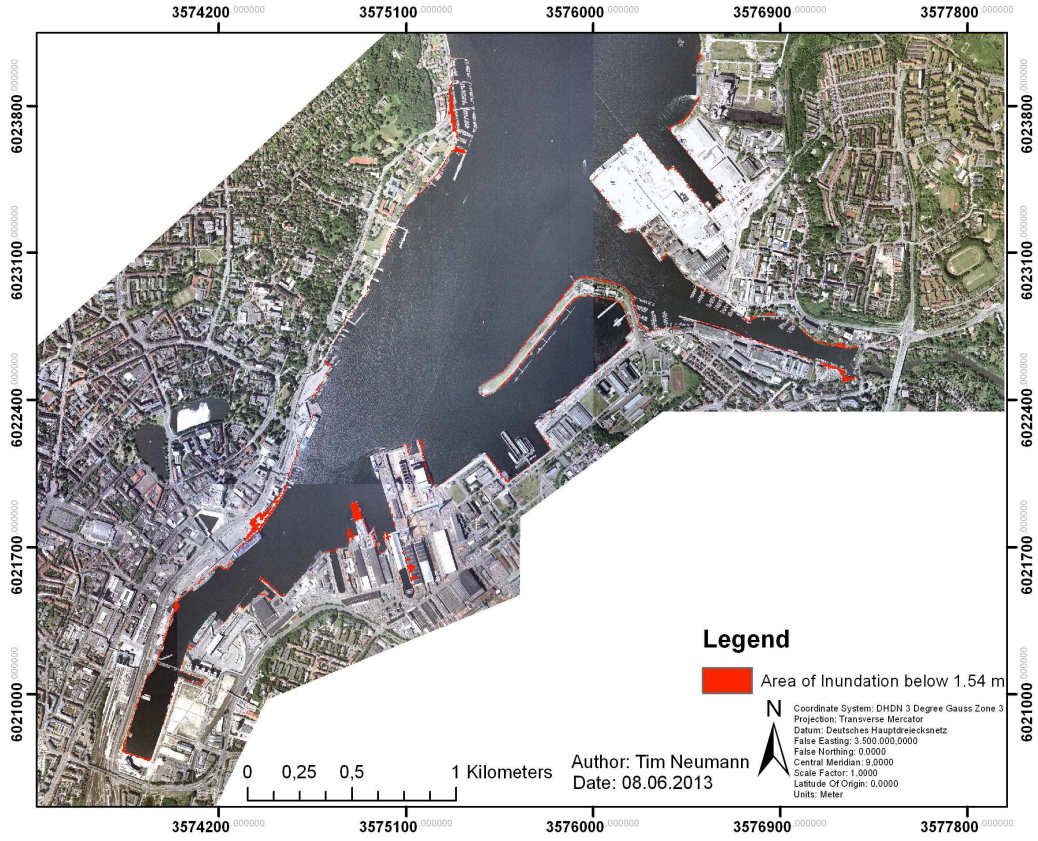


Figure 16: Inundation of Daisy + SLR 0.33m; MWL: 1.54m

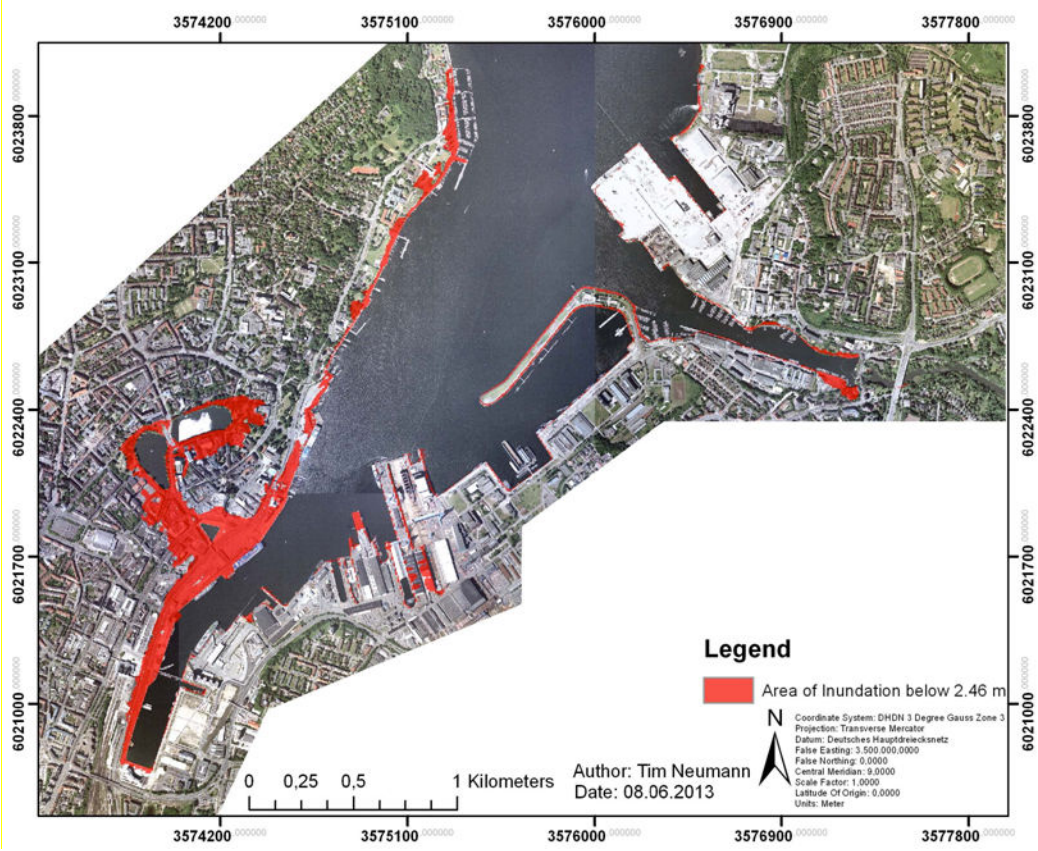


Figure 17: Inundation of Daisy + SLR 1.25m; MWL 2.46m

The maps showed a relatively weak inundation in the lower scenarios. In the scenario of 1.54m it is remarkable that the bigger sized areas of inundation are on the west coast of the

fjord. Also there is a distinct difference for the worst case scenario between the western and eastern waterfront. The trend of the western side is more threaten than the eastern part. Therefore it could be mentioned the most threatening storms are north-easterlies, because of the highest possible fetch for the study area. This provides an even higher risk because the conditions squeeze the water to the western waterfront. Summed up the western part is threaten by two major points, first the general lower elevation in comparison to the eastern part and second higher threatening by natural storm surge conditions. In combination this makes a potential higher risk for the western waterfront.

The following maps are showing the MIKE21 results with a specific choice of cases. Regarding to the presented BTM maps also examples for zero SLR, the additional 0.33m and the 1.25m SLR scenario are displayed. But because for every scenario three runs with different resistances were produced, it will only be shown one each because of the weak differences which are hard to realise on a graphical way. Corresponding to the BTM results, it starts with SLR: 0 and Manning: 32, second is SLR: 0.33m and Manning: 17 and third is SLR: 1.25m and Manning: 12.5.

After showing graphical results of the simulations, a numerical analysis is presented in Tab. 4. The Surface analysis was processed by using the tool 3D-Analyst Tools -Functional Surface -Surface Volume within ArcGIS. It produces results for the area as 2-D and 3-D (taking the DEM into account, to calculate the “real“ surface) and the volume (Rodriguez 2010, pp. 4-5). The here shown Tab. 5 and Tab. 6 are the statistical analysis. Tab. 5 displays the results of the 2-D analysis, Tab. 6 instead represents the 3D analysis as so the "real" surface. Regarding the columns, they show the three different set-ups of resistances for the three different scenarios. The first value would mean BTM underestimates an inundation for a small storm surge of about 1.06 %, if the MIKE21 simulation represents reality.

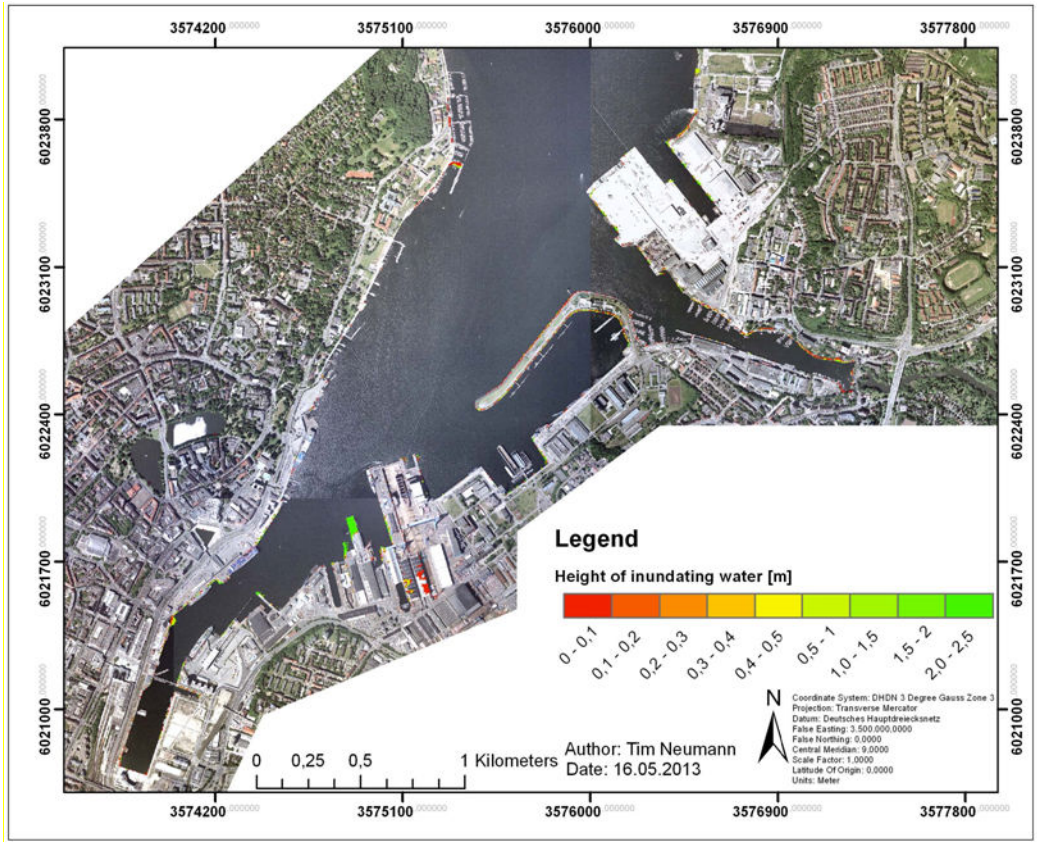


Figure 18: MIKE21 simulation of Daisy; Slr: 0.00m Manning coefficient: 32; MWL: 1.21m

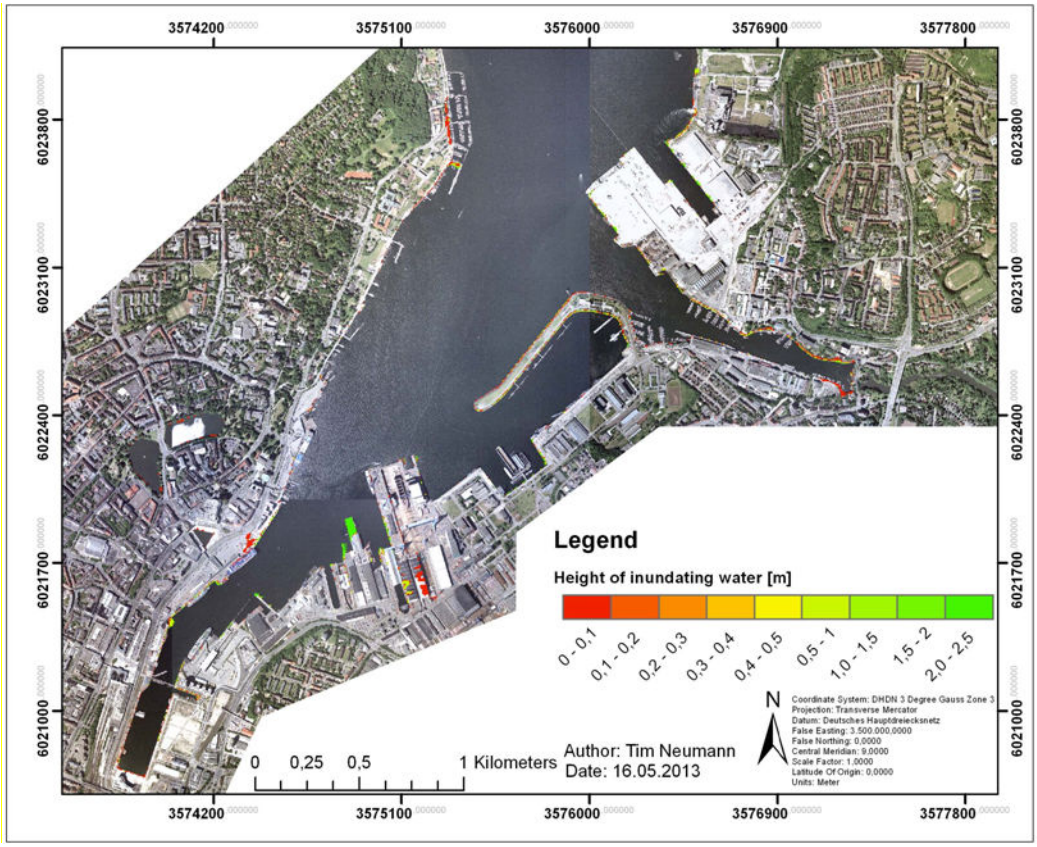


Figure 19: MIKE21 simulation of Daisy; Slr: 0.33m Manning 17, MWL 1.54m

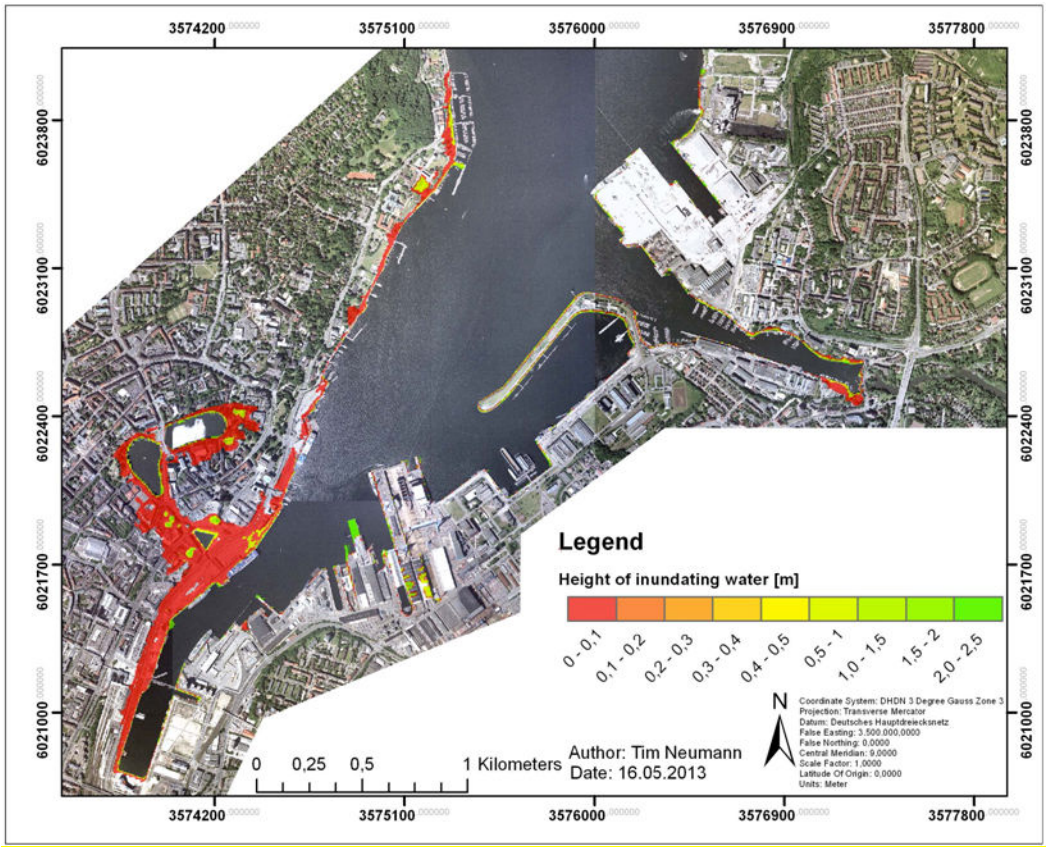


Figure 20: MIKE21 simulation of Daisy; Slr: 1.25m Manning coefficient: 12.5, MWL: 2.46m

Tab. 4: Numerical results of surface analysis in GIS of the three different scenarios applied in ArcGIS and MIKE21 with additional simulation runs on different resistance values

| Approach | Scenario | 2-D Area ($m^2$) | 3-D Area ($m^2$) | Volume of water ($m^3$) |
|---|---|---|---|---|
| BTM | Daisy without SLR (MWL 1.21m) | 7000 | 7672 | 653958.07 |
| | Daisy +0.33m SLR (MWL 1.54m) | 14175 | 14905 | 165043.86 |
| | Daisy +1.25m SLR (MWL 2.46m) | 375550 | 359587 | 5238757.99 |
| MIKE21 | Daisy without SLR; Man. 32 | 7075 | 8027 | 68701.77 |
| | Daisy without SLR; Man. 17 | 7075 | 8027 | 68701.77 |
| | Daisy without SLR; Man. 12.5 | 7075 | 8027 | 68701.77 |
| | Daisy + 0.33m SLR; Man. 32 | 11775 | 12803 | 132999.77 |
| | Daisy + 0.33m SLR; Man. 17 | 11700 | 12729 | 132203.80 |
| | Daisy + 0.33m SLR; Man. 12.5 | 11675 | 12.03 | 131584.39 |
| | Daisy + 1.25m SLR; Man. 32 | 333450 | 336035 | 4869437.55 |
| | Daisy + 1.25m SLR; Man. 17 | 330725 | 333299 | 4828127.38 |
| | Daisy + 1.25m SLR; Man. 12.5 | 325725 | 328293 | 4752628.02 |
| Study Area | Area below 10m | 4030950 | 4052188 | 70513396.93 |

Tab. 5: Relative overestimation of BTM in respect to MIKE21 for 2-D areas

| **Percentage difference of GIS overestimation in comparison to MIKE21 for 2-D area** | | | | | | |
|---|---|---|---|---|---|---|
| **Resistance / SLR (in cm)** | **Manning 32 ($m^{1/3}$ $s^{-1}$)** | **Manning 17 ($m^{1/3}$ $s^{-1}$)** | **Manning 12,5 ($m^{1/3}$ $s^{-1}$)** | **Varying of the resistance values** | **Average difference regarding Resistance** | |
| 0 | -1.06 % | -1.06 % | -1.06 % | 0.00 % | -1.06 % | |
| 33 | 20.38 % | 21.15 % | 21.41 % | 1.03 % | 20.98 % | |
| 125 | 12.63 % | 13.55 % | 15.30 % | 2.67 % | 13.83 % | |
| Average diff. to SLR | 10.65 % | 11.22 % | 11.88 % | | Overall | 11.25 % |

While classifying and evaluating the results, it is important to consider that MIKE21 results were assumed to represent reality, reasoned by the results of the validation in the section hydrodynamic modelling approach. However, to make a reasonable statement, the whole study would have to be validated much more, especially in the context of inundated areas. Therefore a validation like it was done in this work is insufficient, as so all results and assumption are theoretically and cannot be seen as general. Looking to the 2-D analysis, the BTM underestimates the MIKE results in average for a zero SLR by 1.06 %. For the 0.33 SLR and 1.25 scenarios it overestimates MIKE21 by an average of 20.98 % and 13.83%. Respectively to the 3-D analysis BTM underestimates the zero SLR scenario of 4.42 %. But there is an overestimation for the 0.33m SLR and for 1.25m SLR scenario of 16.95 % and 8.14 %. This leads to an overall overestimation by the BTM in comparison to MIKE21 for 2-D of 11.25% and for 3-D of 6.89% respectively.

Tab. 6: Relative overestimation of BTM in respect to MIKE21 for 3-D areas

| **Percentage difference of GIS overestimation in comparison to MIKE21 for 3-D area** | | | | | | |
|---|---|---|---|---|---|---|
| **Resistance / SLR(in cm)** | **Manning 32 ($m^{1/3}$ $s^{-1}$)** | **Manning 17 ($m^{1/3}$ $s^{-1}$)** | **Manning 12,5 ($m^{1/3}$ $s^{-1}$)** | **Varying of the resistance values** | **Average difference regarding Resistance** | |
| 0 | -4.42 % | -4.42 % | -4.42 % | 0.00 % | -4.42 % | |
| 33 | 16.42 % | 17.09 % | 17.33 % | 0.92 % | 16.95 % | |
| 125 | 7.01 % | 7.89 % | 9.53 % | 2.52 % | 8.14 % | |
| Average diff. to SLR | 6.33 % | 6.85 % | 7.48 % | | Overall | 6.89 % |

# 4 Discussion

Looking on the results it depicts for zero SLR there is a tolerable fitting of both methods, while at higher water-levels the BTM overestimates the MIKE21 distinctly. But it is also remarkable that at the highest scenario the difference between both approaches decreases again. This poses the question for the “why“. To formulate a first conclusion it is needed to recapitulate the key points of both approaches. Summing up the BTM, it assumes the complete area under a certain level as inundated, corrected by processing hydrological connectivity. A HDM instead works on a three part basis, the DEM, the input data and the physics, which calculate the behaviour of DEM and input to each other. Like mentioned above, inundation is a process where a flushing medium gets in interaction with the earth surface. Due to this, there are forces arising e.g. friction. Based on these facts a HDM does not take a certain level as inundated, but it takes certain cells of a grid as flooded if the parameter "flooded" of a particular cell is set positive. Thinking about this it seems to be obvious and let presume, that lower water level conditions are under major influence of physical parameters. Looking on the first scenario, without SLR and MWL of 1.21, it is negligible in this argumentation, because the differences of both approaches are tolerable weak and the affected area is comparatively small.

Looking on the results for the scenario of 1.54 MWL it leads to the assumption that the physical interactions for a relatively low water level like this, are of immense importance. A reason for this could be, if an event of lower water levels takes place, just a shallow water layer reaches the land, like presented in Fig.15 and Fig. 16 the resulting forces by the earth surface on the water body (e.g. friction) are stronger than the pressure gradient of the water which floats water inland. Concerning this, a first conclusion would be that the resulting inundation of the simulation is lower than the BTM assumption because HDm includes physical behaviour of the interaction of water and land. Friction is presumed as a main significant force, influencing inundation.

Considering the results of the simulations under different resistance coefficients a further recognition would be that the meaning of the resistance values itself and the resulting differences in the inundation results are comparatively low. The average differences, regarding the influence of the Manning values varies for the 2-D analysis of about 1.23 % and for the 3-D analysis 1.15 %. Looking at these numbers this would mean that the significance of different Manning values is comparatively weak. What modifies the conclusion to the statement, that it isn't much important for this case-study what particular friction value is taken in the calculation. More significant is to simulate an inundation on basis of physical behaviour. And simplifying this, it is more important to take friction in consideration anyway than concentrating on specific values. But again limitations have to be mentioned. Because the model set-up was relatively basic, differences in resistance factors were not significant.

May be it would be more testable and descriptive if the DEM would be further improved to make it more differentiated and to give specific resistance values to differentiated classes like houses or green areas etc., like done in Kaiser et al. (2011). Considering the results of higher water level a decreasing overestimation is to realise. Areas which are flooded have a weaker resistance than the earth surface itself, because water has a low friction factor (see Tab. 1). It strength the arguing of the before mentioned conclusion, that the differences appear because of the physical interaction, which is included by HDm, and as a primary factor the friction.

This can be further argued as, if an event of higher water regimes reaches land, the relation of the pressure gradient of the water and the counter acting force of the friction changes towards the water flushing land inwards. Due to higher water levels also the relation of the water level in respect to the land elevation decreases, what simplifies the inundation. This difference between the water level and land level is much higher at lower water levels, what makes it more difficult for water to inundate anyway. Due to the higher water and lower resistance, because of inundated areas, it is likely that the now limiting factor is the topography itself instead of the physical behaviour.

That would lead to a second conclusion. Rising water level shifts the significance of the designated forces. Looking at lower water levels, the physical interactions between water and land are the primary forces which determine inundation. While at higher water levels the physical interaction, in the manner of friction influencing inundation decreases. So the determining factor for inundation becomes the topography.

It is very likely that there is still a huge potential to gain precision and to make the study more convincing. Beginning at the DEM which could be more detailed for example by a resolution of 1x1m. Due to less interpolation between points of the DEM the result could become more precise. On the other hand this would lead to immense higher computational costs, and because the SWE is a simplification of reality there has to be further development to resolve micro-processes on a reasonable manner. Otherwise a higher resolution could also lead to wrong results or overload nowadays HDM. It is to mention, that if a higher resolution is desired, it has to be parameterise to keep the demand for resources in a tolerable amount. Another point to gain more precise results was mentioned above, is to differentiate the DEM by certain friction coefficients for different areas. This would may lead to the fastest improvement of the here shown study.

The biggest criticism should be the validation of the inundation. To generate a reasonable analysis there has to be known former inundated areas and validate the model on this basis. Only by doing so, the outcome would be reasonable and meaningful. However, even processing like this, it still has to be considered that the system of equations which work in the HDM are just a simplification of reality and only can show a trend of a result, but no absolute correct numbers.

Regarding this work, the results show a trend which can be taken as conclusion. Due to the fact there are always uncertainties, in this case in the engineering correctness of the DEM due to interpolation, in the hydrological correct calculation of the model due to simplification of the reality and excluding culverts and ditches. To classify the statistical results of the comparison it has to be mentioned, that for a reasonable statement the study has to be repeated on different study areas to give an assessment about the BTM error. To make a statement about the advantages or disadvantages of both approaches it has to be mentioned to use a model like MIKE21 takes a lot of effort and resources e.g. time. Therefore it has to be considered what information is required. It is probable applying a HDm leads to a sounder

understanding of a particular inundation. Therefore it may be should considered to apply a HDM to generate a comparable result to another approach like the BTM.

## References

AMTLICHES TOPOGRAPHISCH-KARTOGRAPHISCHES INFORMATIONSSYSTEM (2008): Digitale Geländemodelle (ATKIS®-DGM) Digitales Geländemodell in verschiedenen Gitterweiten. URL: http://www.schleswig-holstein.de/LVERMGEOSH/DE/Geobasisdaten/AtkisDgm/atkisDgm_node.html (Stand: 09.05.2013)

BALICA, S.F.; POPESCU, I.; BEEVERS, C. & N.G. Wright (2013): Parametric and physically based modelling techniques for flood risk and vulnerability assessment: A comparison. In: Environmental Modelling & Software 41/2013, p. 84-92

BATES, P.D.; DAWSON, R.J.; HALL, J.W.; HORRITT, M.S.; NICHOLLS, R. & WICKS, J. & M. A. A. M. HASSAN (2005): Simplified two-dimensional numerical modelling of coastal flooding and example applications. In: Coastal Engineering 52/2005, p793-810

BSH, BUNDESAMT FÜR SEESCHIFFFAHRT UND HYDROGRAPHY (2013a): Sturmflutberichte. URL: http://www.bsh.de/de/Meeresdaten/Vorhersagen/Sturmfluten/Berichte/Sturmflut_vom_09.-10.01.2010.pdf Stand: 30.04.2013

BSH, BUNDESAMT FÜR SEESCHIFFFAHRT UND HYDROGRAPHY (2013b): Sturmfluten. URL: http://www.bsh.de/de/Meeresdaten/Vorhersagen/Sturmfluten/index.jsp Stand 30.04.2013

CHEUNG, K.F.; PHADKE, A.C.; WEI, Y.; ROJASA, R.; DOUYERE, Y.J.-M.; MARTINO, C.D.; HOUSTON, S.H.; LIU, P.L.-F.; LYNETT, P.J.; DODD, N.; LIAO, S. & E. NAKAZAKI (2003): Modelling of storm-induced coastal flooding for emergency management. In: Ocean Engineering, Vol.30, pp. 1353-1386

COOPER, H.M.; CHEN, Q.; FLETCHER, C.H. & M. M. BARBEE (2013): Assessing vulnerability due to sea-level rise in Maui, Hawai‘i using LiDAR remote sensing and GIS. In: Climatic Change 116/2013, p. 547-563

DHI (DANISH HYDRAULIC INSTITUTE) (2009a):MIKE21 FlOW MODEL. Hydrodynamic module. Scientific Documentation.

DHI (DANISH HYDRAULIC INSTITUTE) (2009b):MIKE21 FlOW MODEL. Hydrodynamic module. User Guide.

GECKELER, C. (Ynr): Silvester for 100 Jahren - Sturmflut in Kiel. URL: http://www.kiel.de/kultur/stadtarchiv/erinnerungstage/?id=28 (Stand: 10.06.2013)

GOLDEN SOFTWARE (2002): Surfer User‘s Guide. Contouring and 3D Surface mapping for Scientists and Engineers. Colorado.

GRAHAM, L.P.; CHEN, D.; CHRISTENSEN, O.B.; KJELLSTRÖM, E.; KRYSANOVA, V.; MEIER, H.E.M.; RADZIJEWSKI, M.; RAISANEN, J.; ROCKEL, B. & K. RUOSTEENOJA (2008): Projections of Future Anthropogenic Climate Change. In: The BACC Author Team: Assessment of Climate Change in the Baltic Sea Basin. Berlin, pp. 133-219

HARRIS, R. & C. JARVIS (2011): Statistics for Geography and Environmental Science. Edinburgh.

IPCC (2007): IPCC Assessment Report 4. Working Group II Report. “Impacts, Adaptation and Vulnerability“. Chapter 6 Coastal systems and low-lying areas. p. 322-325

KAISER, G.; SCHEELE, L.; KORTENHAUS, A.; LOVHOLT, F.; RÖMER, H. & S. LESCHKA (2011): The influence of land cover roughness on the results of high resolution tsunami inundation modelling. In Natural Hazards and Earth System Sciences 11/2011, p. 2521-2540

KLEIN R.J.T & R.J. NICHOLLS (1998): Coastal Zones. In: Handbook on methods for Climate Change Impact Assessment and Adaptation Strategies, p. 177-212

KÖGLER, F.C. & J. ULRICH (1985): Bodengestallten und Sedimente der Kieler Förde. In. Schriften des Naturwissenschaftlichen Vereins für Schleswig-Holstein, pp.1-3. URL: http://www.schriften.uni-kiel.de/Band%2055/Koegler_Ulrich_55_1-33.pdf , (Stand:10.06.2013)

LANDESHAUPTSTADT KIEL (2008): Hochwasserinfo. Interaktive Hochwasserkarte. URL: http://ims.kiel.de/website/www_18_katschu/viewer.htm (Stand: 25.04.2013)

MARKS, K. & P. BATES (2000): Integration of high-resolution topographic data with floodplain flow models. In: Hydrological Processes, Vol.14, pp. 2109-2122

MCKILLUP, S. & M. DARBY DYAR (2010): Geostatistics Explained. An Introductory Guide for Earth Scientists. Cambridge

MUKHERJEE, S.; JOSHI, P.K.; MUKHERJEE, S.; GHOSH, A.; GARG, R.D. & A. MUKHOPADHYAY (2013): Evaluation of vertical accuracy of open source Digital Elevation model (DEM). In: International Journal of Applied Earth Observation and Geo-information 21/2013, pp. 205-217

MUTHUSANKAR, G.; LAKSHUMANAN, C.; PRADEEP-KISHORE, V.; ESWARAMOORTHI, S. & M. P. JONATHAN (2013): Classifying inundation limits in SE coast of India: application of GIS. In: Nat Hazards 65/2013, pp. 2401-2409

NICHOLLS, R.J. & R.J. KLEIN (2005): Climate change and coastal management on Europe‘s coast. In: Vermaat, J. et al. (Hrsg.): managing European Coasts. Past, Present and Future. Berlin/Heidelberg, pp. 199-226

OLIVER, M.A. & A.L. KHARYAT (1999): Investigating the spatial variation of radon in soil geostatistically. GeoComputation Conference. Virginia USA. URL: http:// www.geocomputation.org/1999/095/gc_095.htm Stand: 18.04.2013

POULTER, B. & P.N. HALPIN (2008): Raster modelling of coastal flooding from sea¬ level rise. In: International Journal of Geographical Information Science, Vol.22, No. 2, pp. 167-182

RAYMOND, D.J (YEAR NOT REPORTED): Shallow water equation and the ocean. Professor of Physics and Research Physicist with the Geophysical Research Center at the New Mexico Tech University. URL: http://physics.nmt.edu/~raymond/classes/ph332/ notes/shallowgov/shallowgov.pdf (Stand: 15.04.2013)

REMYA, P.G.; KUMAR, R.; BASU, S. & A. SARKAR (2012): Wave hindcast experiments in the Indian Ocean using MIKE21 SW model. In: Journal of Earth System Science 121, No.2 (2012), pp. 385-392

RODRIGUEZ, A. (2010): Mexican Gulf of Mexico Regional Introduction and Sea Level Rise Analysis of the Carmen Island, Campeche, Mexico Region URL: http:// www.geo.utexas.edu/courses/371c/project/2010S/Projects/Rodriguez.pdf, (Stand: 21.05.2013)

SCHUMACHER, W. (2003): Flutkatastrophen an der deutschen Ostseeküste - Vergangenheit, Gegenwart, Zukunft. Rostock: Redieck & Schade.

SMITH, J. & P. SMITH (2007): environmental modelling. An introduction. Oxford.

SUTHERLAND, J. D.; WALSTRA, J. R.; CHESHE, T. J.; van RIJN, L.C. & H. N. SOUTHGATE (2004): Evaluation of coastal area modelling systems at an estuary mouth. In: Coastal Engineering 51 (2004), p. 119-142

VAN DE SAND, B.; LANSEN, J. & C. HOYNG (2012): Sensitivity of Coastal Flood Risk Assessment to Digital Elevation models. In: Water 4/2012 (ISSN 2073-4441), p. 568-579

WADEY, M.P.; NICHOLLS, R.J. & I. HAIGH (2013): Understanding a coastal flood event: the 10th March 2008 storm surge event in the Solent, UK. In: Natural Hazards, DOI 10.1007/s11069-013-0610-5, pp. 1-26

WAINWRIGHT, J. & M. MULLIGAN (2004): Environmental modelling. Finding Simplicity in Complexity. London

## Data

ATKIS DEM 10x10m provided by Geographical Institute of the University of Kiel

Bathymetrie of the inner Kiel Fjord, provided by BSH

Gauge time series of the Institute Geomar, Maritime Meteorologie, GEOMAR Helmholtz-Zentrum für Ozeanforschung Kiel

Gauge time series of Kiel-Holtenau, Wasser-und Schifffahrtsverwaltung des Bundes (WSV), provided by Bundesanstalt für Gewässerkunde (BfG)

## Abbreviations directory

AOI - area of interest

ATKIS - Amtliches Topographisch-Kartographisches Informations System; stands for: authoritative topographical-cartographical information system

AR - Assessment Report

BTM - "Bathtub Method"

DHI - Danish Hydraulic Institute

GIS - Geographical Information System

GPS - Global Positioning System

HC - Hydrological Connected

HDC - Hydrological Disconnected

HD - Hydro Dynamics

Hdm - Hydro dynamic modelling

HDM - Hydrodynamic Model

IPCC - Intergovernmental Panel on Climate Change

MHHW - Mean Highest High Water

MHW - Mean High Water

MLD - Maximum Lag Distance

MSL - Mean Sea Level

SRES - Special Report Emission Scenarios

SLR - Sea Level Rise

SWE - Shallow Water Equation

TIFF - Tagged Image File Format

WLC - Water Level Change

Ynr - Year not reported

## Impressum

**Herausgeber**
Ecologic Institut gemeinnützige GmbH
Pfalzburger Str. 43/44
10717 Berlin
www.ecologic.eu

**Inhalt erstellt durch:**
Tim Neumann

t.neumann@geographie.uni-kiel.de

**Web**
http://www.klimzug-radost.de



**ISSN** 2192-3140

Das Projekt “Regionale Anpassungsstrategien für die deutsche Ostseeküste“ (RADOST) wird im Rahmen der Maßnahme „Klimawandel in Regionen zukunftsfähig gestalten“ (KLIMZUG) vom Bundesministerium für Bildung und Forschung (BMBF) gefördert

RA:dOst

Regionale Anpassungsstrategien
für die deutsche Ostseeküste

GEFÖRDERT VOM

Bundesministerium
für Bildung
und Forschung

KLIMZUG
Klimawandel in Regionen